



Article

Novel Numerical Investigations of Fuzzy Cauchy Reaction–Diffusion Models via Generalized Fuzzy Fractional Derivative Operators

Manar A. Alqudah ¹, Rehana Ashraf ², Saima Rashid ^{3,*} , Jagdev Singh ⁴, Zakia Hammouch ^{5,6,7} and Thabet Abdeljawad ^{8,9,*}

- ¹ Department Mathematical Sciences, Faculty of Sciences, Princess Nourah Bint Abdulrahman University, P.O. Box 84428, Riyadh 11671, Saudi Arabia; maalqudah@pnu.edu.sa
 - ² Department of Mathematis, Lahore College for Women University, Lahore 54000, Pakistan; rehana.ashraf@jhang.lcwu.edu.pk
 - ³ Department of Mathematics, Government College University, Faisalabad 38000, Pakistan
 - ⁴ Department of Mathematics, JECRC University, Jaipur 303905, Rajasthan, India; jagdevsinghrathore@gmail.com
 - ⁵ Ecole Normale Supérieure de Meknés, Université Moulay Ismail, Meknes 50000, Morocco; hammouch_zakia@tdmu.edu.vn
 - ⁶ Department of Mathematics and Science Education, Harran University, Sanliurfa 63510, Turkey
 - ⁷ Division of Applied Mathematics, Thu Dau Mo University, Thu Dau Mot 75000, Vietnam
 - ⁸ Department of Mathematics and General Sciences, Prince Sultan University, Riyadh 11586, Saudi Arabia
 - ⁹ China Medical University Hospital, China Medical University, Taichung 40402, Taiwan
- * Correspondence: saimarashid@gcuf.edu.pk (S.R.); tabdeljawad@psu.edu.sa (T.A.)



Citation: Alqudah, M.A.; Ashraf, R.; Rashid, S.; Singh, J.; Hammouch, Z.; Abdeljawad, T. Novel Numerical Investigations of Fuzzy Cauchy Reaction–Diffusion Models via Generalized Fuzzy Fractional Derivative Operators. *Fractal Fract.* **2021**, *5*, 151. <https://doi.org/10.3390/fractalfract5040151>

Academic Editors: Xiaoping Xie, Xian-Ming Gu and Maohua Ran

Received: 22 August 2021

Accepted: 28 September 2021

Published: 3 October 2021

Publisher's Note: MDPI stays neutral with regard to jurisdictional claims in published maps and institutional affiliations.



Copyright: © 2021 by the authors. Licensee MDPI, Basel, Switzerland. This article is an open access article distributed under the terms and conditions of the Creative Commons Attribution (CC BY) license (<https://creativecommons.org/licenses/by/4.0/>).

Abstract: The present research correlates with a fuzzy hybrid approach merged with a homotopy perturbation transform method known as the fuzzy Shehu homotopy perturbation transform method (SHPTM). With the aid of Caputo and Atangana–Baleanu under generalized Hukuhara differentiability, we illustrate the reliability of this scheme by obtaining fuzzy fractional Cauchy reaction–diffusion equations (CRDEs) with fuzzy initial conditions (ICs). Fractional CRDEs play a vital role in diffusion and instabilities may develop spatial phenomena such as pattern formation. By considering the fuzzy set theory, the proposed method enables the solution of the fuzzy linear CRDEs to be evaluated as a series of expressions in which the components can be efficiently identified and generating a pair of approximate solutions with the uncertainty parameter $\lambda \in [0, 1]$. To demonstrate the usefulness and capabilities of the suggested methodology, several numerical examples are examined to validate convergence outcomes for the supplied problem. The simulation results reveal that the fuzzy SHPTM is a viable strategy for precisely and accurately analyzing the behavior of a proposed model.

Keywords: Shehu transform; Caputo fractional derivative; AB-fractional operator; homotopy perturbation method; Cauchy reaction–diffusion equation

1. Introduction

Fractional calculus has been acknowledged as a highly valuable framework for addressing sustainability and complex phenomena over the past thirty years due to its advantageous qualities such as its nonlocality, heritability, high reliability, and analyticity [1–7]. The modified fractional notion was developed in order to address the challenges involved with processes including inhomogeneities. Various innovators established the underlying framework, as well as their perspectives on expanding calculus, including Liouville, Hadamard, Caputo, Grunwald, Letnikov, Abel, Riez, Caputo–Fabrizio, Atangana–Baleanu (AB), who researched the use of the fractional derivative and fractional differential equations (FDEs). Numerous essential interactions in electromagnetics, acoustics, viscoelasticity, electrochemistry, and material science are well explained by FDEs [8–20].

Fuzzy set theory is also an effective technique for analyzing unpredictable scenarios. These ambiguities can arise in each part of a fractional equation, such as the ICs and boundary conditions. As a result, when calculating fractional equations in real-world settings, it allows for the implementation of interval or fuzzy formulations. Fuzzy set theory has been widely applied in several domains, i.e., fixed-point theory, topology, fractional calculus, integral inequalities, image processing, bifurcation, control theory, consumer electronics, artificial intelligence, and operations research.

Chang and Zadeh [21] were the first to suggest the fuzzy derivative notion, which was quickly adopted by numerous other researchers [22–24]. Hukuhara's publication [25] is the main focus of the concept of set-valued DEs and fuzzy DEs. The Hukuhara derivative served as the foundation for the investigation of set DEs and, thereafter, fuzzy fractional DEs. Agarwal et al. in [26] reported the fuzzy Riemann–Liouville fractional differential equations leveraging the notion of Hukuhara differentiability, which was the basic foundation for the theme of fuzzy fractional derivatives. To handle ambiguous fractional differential equations, they adopted the Riemann–Liouville differentiability notion, relying on Hukuhara differentiability. The stability analysis of the solution for Riemann–Liouville fuzzy fractional DEs has been expounded in [27,28]. Allahviranloo et al. [29] addressed explicit solutions to unpredictable fractional DEs under Riemann–Liouville \mathcal{H} -differentiability incorporating Mittag–Leffler mechanisms in [30], and formed fuzzy fractional DEs under Riemann–Liouville \mathcal{H} -differentiability and accessed the solution of this model utilizing fuzzy Laplace transforms. They demonstrated two novel existence theorems for fuzzy fractional differential equations using Riemann–Liouville generalized \mathcal{H} -differentiability as well as fuzzy Nagumo and Krasnoselskii–Krein criteria [31]. Bushneq et al. [32] explored the findings of a fuzzy singular integral equation with an Abel type kernel using a novel hybrid method. In [33], Zia et al. adopted a semi-analytical technique for finding the solutions to fuzzy nonlinear integral equations. Salahshour et al. [34] expounded the \mathcal{H} -differentiability with Laplace transform to solve the FDEs. Ahmad et al. [35] studied the third-order fuzzy dispersive PDEs in the Caputo, Caputo–Fabrizio, and Atangana–Baleanu fractional operator frameworks. Shah et al. [36] presented the evolution of one-dimensional fuzzy fractional PDEs.

On this note, we consider the one-dimensional, time-dependent fractional CRDE of relevance as follows:

$$\frac{\partial^\vartheta \Psi(\ell, \mathbf{t}_1)}{\partial \mathbf{t}_1^\vartheta} = \mathcal{D} \frac{\partial^2 \Psi(\ell, \mathbf{t}_1)}{\partial \ell^2} + \mathcal{S}(\ell, \mathbf{t}_1) \Psi(\ell, \mathbf{t}_1), \quad \vartheta \in (0, 1], \quad (1)$$

with the ICs $\Psi(\ell, 0) = g_1(\ell)$, $\ell, \mathbf{t}_1 \in \mathbb{R}$, where Ψ indicates the concentration, \mathcal{S} signifies the reaction parameter, while $\mathcal{D} > 0$ is the diffusion coefficient. Here, ϑ is assumed to be the order of the fractional derivative in the Caputo and Atangana–Baleanu fractional derivatives in the Caputo sense.

Equation (1) has fruitful applications in population dynamics, Allee effect, symbiosis, chemistry, ecology, biology, and physics [37–39]. In [40], Lesnic applied the Adomian decomposition method to find the approximate solutions of CRDEs. Dehghan and Shakeri [41] contemplated the approximate solution of (1) by employing the variational iteration method (VIM). Kumar et al. [42] proposed a modified analytical approach with the existence and uniqueness for fractional equations analogous to (1).

An estimated analytical approach has the advantages of being able to solve complex problems without ascribing motives to numerical solutions to the precise solution to assess its validity. It also has quick estimation accuracy. In [43], a Chinese mathematician, J.-H. He, developed the homotopy perturbation method (HPM) on the premise of homotopy in topology [44]. In HPM, the approximate result is represented as a series that rapidly converges to the exact solution. The versatility of HPM allows it to yield approximate and exact solutions to both linear and nonlinear problems without the necessity for discretization and linearization, as with analytical methods [45]. Various studies have extensively used the HPM to analyze linear and nonlinear PDEs [46–48].

In this research, we employed a hybrid approach of the Shehu transform connected with the homotopy perturbation method for finding the applicability of the fuzzy fractional CRDEs of the type based on prior work. The main objective of this study was to expand the implementation of the SHPTM to develop numerical solutions to fractional CRDEs via fuzziness. The findings of the fractional-order with the uncertainty factor were examined by advanced techniques and methods. The strength of SHPTM is that its value comes from its ability to combine two powerful strategies for obtaining numerical findings for complex equations. Some comparison plots illustrate the supremacy of the Hukuhara generalized fractional derivative of CFD and ABC operators. It is worth noting that the proposed algorithm is capable of reducing the amount of computing costs as compared to conventional systems while maintaining good numerical accuracy maintained by the uncertain term $\lambda \in [0, 1]$. Several physical phenomena can be addressed by the projected method.

2. Basic Notions of Fractional and Fuzzy Calculus

This section clearly exhibits some major features connected to the stream of fuzzy set theory and FC, as well as certain key findings about the Shehu transform. For more details, we refer the reader to [49].

Definition 1 ([50,51]). We say that $\Phi : \mathbb{R} \mapsto [0, 1]$ is a fuzzy set, then it is known to be fuzzy number if it holds the subsequent assumptions:

1. Φ is normal (for some $\eta_0 \in \mathbb{R}; \Phi(\eta_0) = 1$);
2. Φ is upper semi-continuous;
3. $\Phi(\ell_1\zeta + (1 - \zeta)\ell_2) \geq (\Phi(\ell_1) \wedge \Phi(\ell_2)) \forall \zeta \in [0, 1], \ell_1, \ell_2 \in \mathbb{R}$, i.e., Φ is convex;
4. $cl\{\ell \in \mathbb{R}, \Phi(\ell) > 0\}$ is compact.

Definition 2 ([50]). We say that a fuzzy number Φ is λ -level set described as

$$[\Phi]^\lambda = \{\Psi \in \mathbb{R} : \Phi(\Psi) \geq 1\}, \quad (2)$$

where $\lambda \in [0, 1]$ and $\Psi \in \mathbb{R}$.

Definition 3 ([50]). The parameterized version of a fuzzy number is denoted by $[\underline{\Phi}(\lambda), \bar{\Phi}(\lambda)]$ such that $\lambda \in [0, 1]$ satisfies the subsequent assumptions:

1. $\underline{\Phi}(\lambda)$ is non-decreasing, left continuous, bounded over $(0, 1]$ and left continuous at 0;
2. $\bar{\Phi}(\lambda)$ is non-increasing, right continuous, bounded over $(0, 1]$ and right continuous at 0;
3. $\underline{\Phi}(\lambda) \leq \bar{\Phi}(\lambda)$.

Definition 4 ([49]). For $\lambda \in [0, 1]$ and Y to be a scalar, assume that there are two fuzzy numbers $\tilde{\alpha}_1 = (\underline{\alpha}_1, \bar{\alpha}_1)$, $\tilde{\alpha}_2 = (\underline{\alpha}_2, \bar{\alpha}_2)$, then the addition, subtraction and scalar multiplication, respectively, are stated as:

1. $\tilde{\alpha}_1 \oplus \tilde{\alpha}_2 = (\underline{\alpha}_1(\lambda) + \underline{\alpha}_2(\lambda), \bar{\alpha}_1(\lambda) + \bar{\alpha}_2(\lambda));$
2. $\tilde{\alpha}_1 \ominus \tilde{\alpha}_2 = (\underline{\alpha}_1(\lambda) - \underline{\alpha}_2(\lambda), \bar{\alpha}_1(\lambda) - \bar{\alpha}_2(\lambda));$
3. $Y \odot \tilde{\alpha}_1 = \left\{ (Y\underline{\alpha}_1, Y\bar{\alpha}_1) \mid Y \geq 0, (Y\bar{\alpha}_1, Y\underline{\alpha}_1) \mid Y < 0. \right.$

Definition 5 ([34]). Suppose a fuzzy mapping $\Theta : \tilde{E} \times \tilde{E} \mapsto \mathbb{R}$ having two fuzzy numbers $\tilde{\alpha}_1 = (\underline{\alpha}_1, \bar{\alpha}_1)$, $\tilde{\alpha}_2 = (\underline{\alpha}_2, \bar{\alpha}_2)$, then Θ -distance between $\tilde{\alpha}_1$ and $\tilde{\alpha}_2$ is represented as:

$$\Theta(\tilde{\alpha}_1, \tilde{\alpha}_2) = \sup_{\lambda \in [0, 1]} [\max \{|\underline{\alpha}_1(\lambda) - \underline{\alpha}_2(\lambda)|, |\bar{\alpha}_1(\lambda) - \bar{\alpha}_2(\lambda)|\}]. \quad (3)$$

Definition 6 ([34]). Consider a fuzzy mapping $\Xi : \mathbb{R} \mapsto \tilde{E}$, if for any $\epsilon > 0$ there exists $\delta > 0$ and a fixed value of $\mu_0 \in [a_1, a_2]$, we have:

$$\Theta(\Xi(\mu), \Xi(\mu_0)) < \epsilon; \text{ whenever } |\mu - \mu_0| < \delta, \quad (4)$$

then Ξ is known to be continuous.

Definition 7 ([52]). Let $\delta_1, \delta_2 \in \tilde{E}$, if $\delta_3 \in \tilde{E}$ and $\delta_1 = \delta_2 + \delta_3$. The \mathcal{H} -difference δ_3 of δ_1 and δ_2 is denoted as $\delta_1 \ominus^{\mathcal{H}} \delta_2$. Observe that $\delta_1 \ominus^{\mathcal{H}} \delta_2 \neq \delta_1 + (-1)\delta_2$.

Definition 8 ([52]). Suppose that $\Xi : (b_1, b_2) \mapsto \tilde{E}$ and $\tau_0 \in (b_1, b_2)$. Then, Ξ is said to be strongly generalized differentiable at τ_0 if $\Xi'(\tau_0) \in \tilde{E}$ exists such that:

- (i) $\Xi'(\tau_0) = \lim_{h \rightarrow 0} \frac{\Xi(\tau_0+h) \ominus^{\mathcal{H}} \Xi(\tau_0)}{h} = \lim_{h \rightarrow 0} \frac{\Xi(\tau_0) \ominus^{\mathcal{H}} \Xi(\tau_0-h)}{h}$;
- (ii) $\Xi'(\tau_0) = \lim_{h \rightarrow 0} \frac{\Xi(\tau_0) \ominus^{\mathcal{H}} \Xi(\tau_0+h)}{-h} = \lim_{h \rightarrow 0} \frac{\Xi(\tau_0-h) \ominus^{\mathcal{H}} \Xi(\tau_0)}{-h}$.

Throughout this investigation, we use the notation Ξ which is (1)-differentiable and (2)-differentiable, respectively, if it is differentiable under the assumption (i) and (ii) as defined above.

Theorem 1 ([49]). Consider a fuzzy valued function $\Xi : \mathbb{R} \mapsto \tilde{E}$ such that $\Xi(\tau_0; \lambda) = [\underline{\Xi}(\tau_0; \lambda), \bar{\Xi}(\tau_0; \lambda)]$ and $\lambda \in [0, 1]$. Then:

I. $\underline{\Xi}(\tau_0; \lambda)$ and $\bar{\Xi}(\tau_0; \lambda)$ are differentiable, if Ξ is a (1)-differentiable, and:

$$[\Xi'(\tau_0)]^\lambda = [\underline{\Xi}'(\tau_0; \lambda), \bar{\Xi}'(\tau_0; \lambda)]. \tag{5}$$

II. $\underline{\Xi}(\tau_0; \lambda)$ and $\bar{\Xi}(\tau_0; \lambda)$ are differentiable, if Ξ is a (2)-differentiable, and:

$$[\Xi'(\tau_0)]^\lambda = [\bar{\Xi}'(\tau_0; \lambda), \underline{\Xi}'(\tau_0; \lambda)]. \tag{6}$$

Definition 9 ([34]). Assume that a fuzzy mapping $\Psi_{g\mathcal{H}}^{(r)} = \Psi^{(r)} \in \mathbb{C}^F[0, s] \cap \mathbb{L}^F[0, s]$. Then, the fuzzy $g\mathcal{H}$ -fractional Caputo differentiability of fuzzy-valued mapping Ψ is represented as

$$\begin{aligned} ({}^c_{g\mathcal{H}}\mathcal{D}^\vartheta \Psi)(\mathbf{t}_1) &= \mathcal{J}_{a_1}^{r-\vartheta} \odot (\Psi^{(r)})(\tau) \\ &= \frac{1}{\Gamma(r-\vartheta)} \odot \int_{a_1}^{\mathbf{t}_1} (\mathbf{t}_1 - \ell)^{r-\vartheta-1} \odot \Psi^{(r)}(\ell) d\ell, \quad \vartheta \in (r-1, r], r \in \mathbb{N}, \mathbf{t}_1 > a_1. \end{aligned} \tag{7}$$

Therefore, the parameterized versions of $\Psi = [\underline{\Psi}_\lambda(\mathbf{t}_1), \bar{\Psi}_\lambda(\mathbf{t}_1)]$, $\lambda \in [0, 1]$ and $\mathbf{t}_{10} \in (0, s)$, and CFD in a fuzzy sense is stated as

$$[\mathcal{D}_{(i)-g\mathcal{H}}^\vartheta \Psi(\mathbf{t}_{10})]_\lambda = [\mathcal{D}_{(i)-g\mathcal{H}}^\vartheta \underline{\Psi}(\mathbf{t}_{10}), \mathcal{D}_{(i)-g\mathcal{H}}^\vartheta \bar{\Psi}(\mathbf{t}_{10})], \quad \lambda \in [0, 1], \tag{8}$$

where $r = [\lambda]$:

$$\begin{aligned} [\mathcal{D}_{(i)-g\mathcal{H}}^\vartheta \underline{\Psi}(\mathbf{t}_{10})] &= \frac{1}{\Gamma(r-\vartheta)} \left[\int_0^{\mathbf{t}_1} (\mathbf{t}_1 - \mathbf{x})^{r-\vartheta-1} \frac{d^r}{d\mathbf{x}^r} \underline{\Psi}_{(i)-g\mathcal{H}}(\mathbf{x}) d\mathbf{x} \right]_{\mathbf{t}_1=\mathbf{t}_{10}}, \\ [\mathcal{D}_{(i)-g\mathcal{H}}^\vartheta \bar{\Psi}(\mathbf{t}_{10})] &= \frac{1}{\Gamma(r-\vartheta)} \left[\int_0^{\mathbf{t}_1} (\mathbf{t}_1 - \mathbf{x})^{r-\vartheta-1} \frac{d^r}{d\mathbf{x}^r} \bar{\Psi}_{(i)-g\mathcal{H}}(\mathbf{x}) d\mathbf{x} \right]_{\mathbf{t}_1=\mathbf{t}_{10}}. \end{aligned} \tag{9}$$

Definition 10. Assume that a fuzzy mapping $\tilde{\Psi}(\mathbf{t}_1) \in \tilde{\mathbb{H}}^1(0, T)$ and $\vartheta \in [0, 1]$, then the fuzzy $g\mathcal{H}$ -fractional Atangana–Baleanu differentiability of fuzzy-valued mapping is represented as

$$({}_{g\mathcal{H}}\mathcal{D}^\vartheta \Psi)(\mathbf{t}_1) = \frac{\mathbb{B}(\vartheta)}{1-\vartheta} \odot \left[\int_0^{\mathbf{t}_1} \Psi'(\mathbf{x}) \odot E_\vartheta \left[\frac{-\vartheta(\mathbf{t}_1 - \mathbf{x})^\vartheta}{1-\vartheta} \right] d\mathbf{x} \right]. \tag{10}$$

Thus, the parameterized formulation of $\Psi = [\underline{\Psi}_\lambda(\mathbf{t}_1), \bar{\Psi}_\lambda(\mathbf{t}_1)]$, $\lambda \in [0, 1]$ and $\mathbf{t}_0 \in (0, s)$, and the fuzzy Atangana–Baleanu derivative in Caputo sense is stated as

$$\left[{}^{ABC}\mathcal{D}_{(i)-g\mathcal{H}}^\vartheta \tilde{\Psi}(\mathbf{t}_0; \lambda) \right] = \left[{}^{ABC}\mathcal{D}_{(i)-g\mathcal{H}}^\vartheta \underline{\Psi}(\mathbf{t}_0; \lambda), {}^{ABC}\mathcal{D}_{(i)-g\mathcal{H}}^\vartheta \bar{\Psi}(\mathbf{t}_0; \lambda) \right], \quad \lambda \in [0, 1], \quad (11)$$

where:

$$\begin{aligned} {}^{ABC}\mathcal{D}_{(i)-g\mathcal{H}}^\vartheta \underline{\Psi}(\mathbf{t}_0; \lambda) &= \frac{\mathbb{B}(\vartheta)}{1-\vartheta} \left[\int_0^{\mathbf{t}_1} \underline{\Psi}'_{(i)-g\mathcal{H}}(\mathbf{x}) E_\vartheta \left[\frac{-\vartheta(\mathbf{t}_1 - \mathbf{x})^\vartheta}{1-\vartheta} \right] d\mathbf{x} \right]_{\mathbf{t}_1=\mathbf{t}_0}, \\ {}^{ABC}\mathcal{D}_{(i)-g\mathcal{H}}^\vartheta \bar{\Psi}(\mathbf{t}_0; \lambda) &= \frac{\mathbb{B}(\vartheta)}{1-\vartheta} \left[\int_0^{\mathbf{t}_1} \bar{\Psi}'_{(i)-g\mathcal{H}}(\mathbf{x}) E_\vartheta \left[\frac{-\vartheta(\mathbf{t}_1 - \mathbf{x})^\vartheta}{1-\vartheta} \right] d\mathbf{x} \right]_{\mathbf{t}_1=\mathbf{t}_0}, \end{aligned} \quad (12)$$

where $\mathbb{B}(\vartheta)$ denotes the normalized function which is equal to 1 when ϑ is assumed to be 0 and 1. Furthermore, we suppose that type (i) – $g\mathcal{H}$ exists. Thus, here there is no need to consider (ii) – $g\mathcal{H}$ differentiability.

Definition 11 ([53]). Consider a continuous real-valued mapping $\tilde{\Psi}$ and there is an improper fuzzy Riemann-integrable mapping $\exp\left(\frac{-\xi}{\nu}\right) \odot \tilde{\Psi}(\mathbf{t}_1)$ on $[0, +\infty)$. Then, the integral $\int_0^{+\infty} \exp\left(\frac{-\xi}{\nu}\right) \odot \tilde{\Psi}(\mathbf{t}_1) d\mathbf{t}_1$ is known to be the fuzzy Shehu transform and it is stated over the set of mappings:

$$\mathcal{S} = \left\{ \tilde{\Psi}(\mathbf{t}_1) : \exists \mathcal{A}, p_1, p_2 > 0, |\tilde{\Psi}(\mathbf{t}_1)| < \mathcal{A} \exp\left(\frac{|\mathbf{t}_1|}{\zeta_j}\right), \text{ if } \mathbf{t}_1 \in (-1)^j \times [0, +\infty) \right\}, \quad (13)$$

as

$$\mathcal{S}[\tilde{\Psi}(\mathbf{t}_1)] = \mathcal{S}(\xi, \nu) = \int_0^{+\infty} \exp\left(\frac{-\xi}{\nu} \mathbf{t}_1\right) \odot \tilde{\Psi}(\mathbf{t}_1) d\mathbf{t}_1, \quad \xi, \nu > 0. \quad (14)$$

Remark 1. In (14), $\tilde{\Psi}$ fulfills the assumption of the decreasing diameter $\underline{\Psi}$ and increasing diameter $\bar{\Psi}$ of a fuzzy mapping Ψ . If $\nu = 1$, then fuzzy the Shehu transform is reduced to fuzzy Laplace transform.

Using the fact of Salahshour et al. [30], we have:

$$\int_0^{+\infty} \exp\left(\frac{-\xi}{\nu} \mathbf{t}_1\right) \odot \tilde{\Psi}(\mathbf{t}_1) d\mathbf{t}_1 = \left(\int_0^{+\infty} \exp\left(\frac{-\xi}{\nu} \mathbf{t}_1\right) \underline{\Psi}(\mathbf{t}_1; \lambda) d\mathbf{t}_1, \int_0^{+\infty} \exp\left(\frac{-\xi}{\nu} \mathbf{t}_1\right) \bar{\Psi}(\mathbf{t}_1; \lambda) d\mathbf{t}_1 \right). \quad (15)$$

Furthermore, considering the classical Shehu transform [54], we obtain:

$$\mathcal{S}[\underline{\Psi}(\mathbf{t}_1; \lambda)] = \int_0^{+\infty} \exp\left(\frac{-\xi}{\nu} \mathbf{t}_1\right) \underline{\Psi}(\mathbf{t}_1; \lambda) d\mathbf{t}_1 \quad (16)$$

and:

$$\mathcal{S}[\bar{\Psi}(\mathbf{t}_1; \lambda)] = \int_0^{+\infty} \exp\left(\frac{-\xi}{\nu} \mathbf{t}_1\right) \bar{\Psi}(\mathbf{t}_1; \lambda) d\mathbf{t}_1. \quad (17)$$

Then, the aforesaid expressions can be written as

$$\begin{aligned}\mathbf{S}[\tilde{\Psi}(\mathbf{t}_1)] &= \left(\mathbf{S}[\underline{\Psi}(\mathbf{t}_1; \lambda)], \mathbf{S}[\bar{\Psi}(\mathbf{t}_1; \lambda)] \right) \\ &= \left(\underline{\mathcal{S}}(\xi, \nu), \bar{\mathcal{S}}(\xi, \nu) \right).\end{aligned}\quad (18)$$

Then, we will define the fuzzy Shehu transform of the Caputo generalized Hukuhara derivative ${}^c_{g\mathcal{H}}\mathcal{D}_{\mathbf{t}_1}^\vartheta \Psi(\mathbf{t}_1)$, as can be seen in [53].

Definition 12 ([53]). Suppose there is an integrable fuzzy-valued mapping ${}^c_{g\mathcal{H}}\mathcal{D}_{\mathbf{t}_1}^\vartheta \tilde{\Psi}(\mathbf{t}_1)$, and $\Psi(\mathbf{t}_1)$ is the primitive of ${}^c_{g\mathcal{H}}\mathcal{D}_{\mathbf{t}_1}^\vartheta \tilde{\Psi}(\mathbf{t}_1)$ on $[0, +\infty)$, then the CFD of order ϑ is presented as

$$\mathbf{S}[{}^c_{g\mathcal{H}}\mathcal{D}_{\mathbf{t}_1}^\vartheta \tilde{\Psi}(\mathbf{t}_1)] = \left(\frac{\xi}{\nu}\right)^\vartheta \odot \mathbf{S}[\tilde{\Psi}(\mathbf{t}_1)] \ominus \sum_{\kappa=0}^{r-1} \left(\frac{\xi}{\nu}\right)^{\vartheta-\kappa-1} \odot \tilde{\Psi}^{(\kappa)}(0), \quad \vartheta \in (r-1, r]. \quad (19)$$

Again, using the fact of Salahshour et al. [30], we have:

$$\begin{aligned}&\left(\frac{\xi}{\nu}\right)^\vartheta \odot \mathbf{S}[\tilde{\Psi}(\mathbf{t}_1)] \ominus \sum_{\kappa=0}^{r-1} \left(\frac{\xi}{\nu}\right)^{\vartheta-\kappa-1} \odot \tilde{f}^{(\kappa)}(0) \\ &= \left(\left(\frac{\xi}{\nu}\right)^\vartheta \mathbf{S}[\underline{\Psi}(\mathbf{t}_1; \lambda)] - \sum_{\kappa=0}^{r-1} \left(\frac{\xi}{\nu}\right)^{\vartheta-\kappa-1} \odot \underline{\Psi}^{(\kappa)}(0; \lambda), \left(\frac{\xi}{\nu}\right)^\vartheta \mathbf{S}[\bar{\Psi}(\mathbf{t}_1; \lambda)] - \sum_{\kappa=0}^{r-1} \left(\frac{\xi}{\nu}\right)^{\vartheta-\kappa-1} \bar{\Psi}^{(\kappa)}(0; \lambda) \right).\end{aligned}$$

Bokhari et al. [55] defined the ABC fractional derivative operator in the Shehu sense. Furthermore, we extend the idea of fuzzy ABC fractional derivative in a fuzzy Shehu transform sense as follows:

Definition 13. Consider $\Psi \in \mathbb{C}^F[0, s] \cap \mathbb{L}^F[0, s]$ such that $\tilde{\Psi}(\mathbf{t}_1) = [\underline{\Psi}(\mathbf{t}_1, \lambda), \bar{\Psi}(\mathbf{t}_1, \lambda)]$, $\lambda \in [0, 1]$; then, the Shehu transform of the fuzzy ABC of order $\vartheta \in [0, 1]$ is described as follows:

$$\mathbf{S}[{}_{g\mathcal{H}}\mathcal{D}_{\mathbf{t}_1}^\vartheta \tilde{\Psi}(\mathbf{t}_1)] = \frac{\mathbb{B}(\vartheta)}{1 - \vartheta + \vartheta\left(\frac{\nu}{\xi}\right)^\vartheta} \odot \left(\tilde{\mathbf{V}}(\nu, \xi) \ominus \frac{\nu}{\xi} \tilde{\Psi}(0) \right). \quad (20)$$

Furthermore, using the fact of Salahshour et al. [30], we have:

$$\begin{aligned}&\frac{\mathbb{B}(\vartheta)}{1 - \vartheta + \vartheta\left(\frac{\nu}{\xi}\right)^\vartheta} \odot \left(\tilde{\mathbf{V}}(\nu, \xi) \ominus \frac{\nu}{\xi} \tilde{\Psi}(0) \right) \\ &= \left(\frac{\mathbb{B}(\vartheta)}{1 - \vartheta + \vartheta\left(\frac{\nu}{\xi}\right)^\vartheta} \left(\underline{\mathbf{V}}(\nu, \xi; \lambda) - \frac{\nu}{\xi} \underline{\Psi}(0; \lambda) \right), \frac{\mathbb{B}(\vartheta)}{1 - \vartheta + \vartheta\left(\frac{\nu}{\xi}\right)^\vartheta} \left(\bar{\mathbf{V}}(\nu, \xi; \lambda) - \frac{\nu}{\xi} \bar{\Psi}(0; \lambda) \right) \right).\end{aligned}\quad (21)$$

3. Description of the Fuzzy SHPTM

In this unit, we exhibit the fundamental technique of the fuzzy SHPTM to establish the general solution for the one-dimensional fuzzy fractional Cauchy reaction–diffusion equation.

Here, we employ the following generic form of the time-fractional fuzzy PDE to implement this technique:

$${}^*\mathcal{D}_{\mathbf{t}_1}^\vartheta \tilde{\Psi}(\ell, \mathbf{t}_1; \lambda) \oplus \mathcal{L}\langle \tilde{\Psi}(\ell, \mathbf{t}_1; \lambda) \rangle \oplus \mathcal{N}\langle \tilde{\Psi}(\ell, \mathbf{t}_1; \lambda) \rangle = \theta(\ell, \mathbf{t}_1; \lambda), \quad \mathbf{t}_1 > 0, \quad r-1 < \vartheta \leq r, \quad (22)$$

subject to:

$$\tilde{\Psi}^{(\kappa)}(\ell, 0; \lambda) = \tilde{g}_\kappa(\ell; \lambda), \quad \kappa = 0, 1, 2, \dots, r-1. \quad (23)$$

The parameterized formulation of (22) is exhibited as

$$\begin{cases} {}_0^* \mathcal{D}_{\mathbf{t}_1}^\vartheta \underline{\Psi}(\ell, \mathbf{t}_1; \lambda) + \mathcal{L}\langle \underline{\Psi}(\ell, \mathbf{t}_1; \lambda) \rangle + \mathcal{N}\langle \underline{\Psi}(\ell, \mathbf{t}_1; \lambda) \rangle = \theta(\ell, \mathbf{t}_1; \lambda), & r-1 < \vartheta \leq r, \\ \tilde{\Psi}(\ell, 0) = \tilde{g}(\ell; \lambda), \\ {}_0^* \mathcal{D}_{\mathbf{t}_1}^\vartheta \underline{\Psi}(\ell, \mathbf{t}_1; \lambda) + \mathcal{L}\langle \underline{\Psi}(\ell, \mathbf{t}_1; \lambda) \rangle + \mathcal{N}\langle \underline{\Psi}(\ell, \mathbf{t}_1; \lambda) \rangle = \theta(\ell, \mathbf{t}_1; \lambda), & r-1 < \vartheta \leq r, \\ \tilde{\Psi}(\ell, 0) = \tilde{g}(\ell; \lambda). \end{cases} \quad (24)$$

where ${}_0^* \mathcal{D}_{\mathbf{t}_1}^\vartheta$ represents the CFD or AB fractional derivative in the Caputo sense and the linear term is denoted by $\mathcal{L}\langle \cdot \rangle$ and the nonlinear factor is denoted by $\mathcal{N}\langle \cdot \rangle$. Taking into consideration the fuzzy Shehu transform elaborated in Definition 12 and Definition 13, respectively, we characterize the iterative process for the solution of (22). For this, we proceed with the first case of (24) and transformed mappings for the fuzzy CFD operator, then for fuzzy AB fractional derivative in the Caputo sense as

$$\left(\frac{\nu}{\xi}\right)^\vartheta \mathbf{S}[\underline{\Psi}(\ell, \mathbf{t}_1; \lambda)] - \sum_{\kappa=0}^{r-1} \left(\frac{\xi}{\nu}\right)^{\vartheta-\kappa-1} \underline{\Psi}^{(\kappa)}(0) = \mathbf{S}[\mathcal{L}\langle \underline{\Psi}(\ell, \mathbf{t}_1; \lambda) \rangle + \mathcal{N}\langle \underline{\Psi}(\ell, \mathbf{t}_1; \lambda) \rangle] + \mathbf{S}[\theta(\ell, \mathbf{t}_1; \lambda)].$$

Furthermore, the transformed function in the fuzzy ABC derivative sense:

$$\begin{aligned} & \frac{\mathbb{B}(\vartheta)}{1-\vartheta+\vartheta\left(\frac{\nu}{\xi}\right)^\vartheta} \mathbf{S}[\underline{\Psi}(\ell, \mathbf{t}_1; \lambda)] - \frac{\mathbb{B}(\vartheta)}{1-\vartheta+\vartheta\left(\frac{\nu}{\xi}\right)^\vartheta} \left(\frac{\nu}{\xi}\right)^\vartheta \underline{\Psi}(\ell, 0) \\ & = \mathbf{S}[\mathcal{L}\langle \underline{\Psi}(\ell, \mathbf{t}_1; \lambda) \rangle + \mathcal{N}\langle \underline{\Psi}(\ell, \mathbf{t}_1; \lambda) \rangle] + \mathbf{S}[\theta(\ell, \mathbf{t}_1; \lambda)]. \end{aligned}$$

It follows that:

$$\mathbf{S}[\underline{\Psi}(\ell, \mathbf{t}_1; \lambda)] = \mathcal{G}_1(\ell, \mathbf{t}_1; \lambda) + \left(\frac{\nu}{\xi}\right)^\vartheta \mathbf{S}[\mathcal{L}\langle \underline{\Psi}(\ell, \mathbf{t}_1; \lambda) \rangle + \mathcal{N}\langle \underline{\Psi}(\ell, \mathbf{t}_1; \lambda) \rangle], \quad (25)$$

and:

$$\mathbf{S}[\underline{\Psi}(\ell, \mathbf{t}_1; \lambda)] = \mathcal{G}_1(\ell, \mathbf{t}_1; \lambda) + \left(\frac{\nu}{\xi}\right)^\vartheta \underline{\Psi}(\ell, 0) + \left(\frac{1-\vartheta+\vartheta\left(\frac{\nu}{\xi}\right)^\vartheta}{\mathbb{B}(\vartheta)}\right) \mathbf{S}[\mathcal{L}\langle \underline{\Psi}(\ell, \mathbf{t}_1; \lambda) \rangle + \mathcal{N}\langle \underline{\Psi}(\ell, \mathbf{t}_1; \lambda) \rangle], \quad (26)$$

where $\mathcal{G}_1(\ell, \mathbf{t}_1; \lambda) = \left(\frac{\nu}{\xi}\right)^\vartheta \underline{\Psi}(\ell, 0) + \left(\frac{\nu}{\xi}\right)^\vartheta \mathbf{S}[\theta(\ell, \mathbf{t}_1; \lambda)]$ and $\mathcal{G}_2(\ell, \mathbf{t}_1; \lambda) = \left(\frac{\nu}{\xi}\right)^\vartheta \underline{\Psi}(\ell, 0) + \left(\frac{1-\vartheta+\vartheta\left(\frac{\nu}{\xi}\right)^\vartheta}{\mathbb{B}(\vartheta)}\right) \mathbf{S}[\theta(\ell, \mathbf{t}_1; \lambda)]$, respectively. By employing the perturbation method, we acquire the solution of the first case of (24) as

$$\underline{\Psi}(\ell, \mathbf{t}_1; \lambda) = \sum_{\kappa=0}^{+\infty} \eta^\kappa \underline{\Psi}_\kappa(\ell, \mathbf{t}_1; \lambda), \quad \kappa = 0, 1, 2, \dots \quad (27)$$

The nonlinear term in (24) can be calculated from:

$$\mathcal{N}\langle \underline{\Psi}(\ell, \mathbf{t}_1; \lambda) \rangle = \sum_{\kappa=0}^{+\infty} \eta^\kappa \mathbf{F}_\kappa(\ell, \mathbf{t}_1; \lambda) \quad (28)$$

and the components of: $\underline{\mathbf{F}}_\kappa(\ell, \mathbf{t}_1; \lambda)$ are the He's polynomials [56] as

$$\underline{\mathbf{F}}_\kappa(\underline{\Psi}_0, \underline{\Psi}_1, \dots, \underline{\Psi}_\kappa) = \frac{1}{\kappa!} \frac{\partial^\kappa}{\partial \zeta^\kappa} \left[\mathcal{N} \left(\sum_{\kappa=0}^{+\infty} \zeta^\kappa \underline{\Psi}_\kappa \right) \right]_{\zeta=0}, \quad \kappa = 0, 1, 2, \dots \quad (29)$$

Substituting (27) and (28) into (25), we attain the iterative terms which yield the solution for the fuzzy fractional CFD operator:

$$\sum_{\kappa=0}^{+\infty} \eta^\kappa \underline{\Psi}_\kappa(\ell, \mathbf{t}_1; \lambda) = \mathcal{G}_1(\ell, \mathbf{t}_1; \lambda) + \eta \left(\frac{\nu}{\xi} \right)^\vartheta \left[\mathbf{S} \left\{ \mathcal{L} \left\langle \sum_{\kappa=0}^{+\infty} \eta^\kappa \underline{\Psi}_\kappa(\ell, \mathbf{t}_1; \lambda) \right\rangle + \sum_{\kappa=0}^{+\infty} \eta^\kappa \underline{\mathbf{F}}_\kappa(\ell, \mathbf{t}_1; \lambda) \right\} \right], \quad (30)$$

and again, plugging (27) and (29) into (26), we attain the iterative terms which yield the solution for the fuzzy AB fractional derivative operator in the Caputo sense:

$$\sum_{\kappa=0}^{+\infty} \eta^\kappa \underline{\Psi}_\kappa(\ell, \mathbf{t}_1; \lambda) = \mathcal{G}_2(\ell, \mathbf{t}_1; \lambda) + \eta \left(\frac{1 - \vartheta + \vartheta \left(\frac{\nu}{\xi} \right)^\vartheta}{\mathbb{B}(\vartheta)} \right) \left[\mathbf{S} \left\{ \mathcal{L} \left\langle \sum_{\kappa=0}^{+\infty} \eta^\kappa \underline{\Psi}_\kappa(\ell, \mathbf{t}_1; \lambda) \right\rangle + \sum_{\kappa=0}^{+\infty} \eta^\kappa \underline{\mathbf{F}}_\kappa(\ell, \mathbf{t}_1; \lambda) \right\} \right]. \quad (31)$$

Then, by equating powers of η in (30), we compute the following CFD homotopies:

$$\begin{aligned} \eta^0 : \underline{\Psi}_0(\ell, \mathbf{t}_1; \lambda) &= \mathcal{G}_1(\ell, \mathbf{t}_1; \lambda) = \left(\frac{\nu}{\xi} \right) \underline{\Psi}(\ell, 0) + \left(\frac{\nu}{\xi} \right)^\vartheta \mathbf{S}[\theta(\ell, \mathbf{t}_1; \lambda)], \\ \eta^1 : \underline{\Psi}_1(\ell, \mathbf{t}_1; \lambda) &= \left(\frac{\nu}{\xi} \right)^\vartheta \mathbf{S} \left\{ \mathcal{L} \langle \underline{\Psi}_0(\ell, \mathbf{t}_1; \lambda) \rangle + \underline{\mathbf{F}}_0(\ell, \mathbf{t}_1; \lambda) \right\}, \\ \eta^2 : \underline{\Psi}_2(\ell, \mathbf{t}_1; \lambda) &= \left(\frac{\nu}{\xi} \right)^\vartheta \mathbf{S} \left\{ \mathcal{L} \langle \underline{\Psi}_1(\ell, \mathbf{t}_1; \lambda) \rangle + \underline{\mathbf{F}}_1(\ell, \mathbf{t}_1; \lambda) \right\}, \\ &\vdots \\ \eta^{\kappa+1} : \underline{\Psi}_{\kappa+1}(\ell, \mathbf{t}_1; \lambda) &= \left(\frac{\nu}{\xi} \right)^\vartheta \mathbf{S} \left\{ \mathcal{L} \langle \underline{\Psi}_\kappa(\ell, \mathbf{t}_1; \lambda) \rangle + \underline{\mathbf{F}}_\kappa(\ell, \mathbf{t}_1; \lambda) \right\}. \end{aligned} \quad (32)$$

Moreover, by equating powers of η in (31), we compute the following ABC operator homotopies:

$$\begin{aligned} \eta^0 : \underline{\Psi}_0(\ell, \mathbf{t}_1; \lambda) &= \mathcal{G}_2(\ell, \mathbf{t}_1; \lambda) = \left(\frac{\nu}{\xi} \right) \underline{\Psi}(\ell, 0) + \left(\frac{1 - \vartheta + \vartheta \left(\frac{\nu}{\xi} \right)^\vartheta}{\mathbb{B}(\vartheta)} \right) \mathbf{S}[\theta(\ell, \mathbf{t}_1; \lambda)], \\ \eta^1 : \underline{\Psi}_1(\ell, \mathbf{t}_1; \lambda) &= \left(\frac{1 - \vartheta + \vartheta \left(\frac{\nu}{\xi} \right)^\vartheta}{\mathbb{B}(\vartheta)} \right) \mathbf{S} \left\{ \mathcal{L} \langle \underline{\Psi}_0(\ell, \mathbf{t}_1; \lambda) \rangle + \underline{\mathbf{F}}_0(\ell, \mathbf{t}_1; \lambda) \right\}, \\ \eta^2 : \underline{\Psi}_2(\ell, \mathbf{t}_1; \lambda) &= \left(\frac{1 - \vartheta + \vartheta \left(\frac{\nu}{\xi} \right)^\vartheta}{\mathbb{B}(\vartheta)} \right) \mathbf{S} \left\{ \mathcal{L} \langle \underline{\Psi}_1(\ell, \mathbf{t}_1; \lambda) \rangle + \underline{\mathbf{F}}_1(\ell, \mathbf{t}_1; \lambda) \right\}, \\ &\vdots \\ \eta^{\kappa+1} : \underline{\Psi}_{\kappa+1}(\ell, \mathbf{t}_1; \lambda) &= \left(\frac{1 - \vartheta + \vartheta \left(\frac{\nu}{\xi} \right)^\vartheta}{\mathbb{B}(\vartheta)} \right) \mathbf{S} \left\{ \mathcal{L} \langle \underline{\Psi}_\kappa(\ell, \mathbf{t}_1; \lambda) \rangle + \underline{\mathbf{F}}_\kappa(\ell, \mathbf{t}_1; \lambda) \right\}, \end{aligned} \quad (33)$$

After applying the inverse Shehu transform, the components of $\underline{\Psi}_\kappa(\ell, \mathbf{t}_1; \lambda)$ are easily computed to the convergence series form, when $\eta \rightarrow 1$; thus, we acquire the approximate solution of (22):

$$\begin{aligned} \underline{\Psi}(\ell, \mathbf{t}_1; \lambda) \approx \underline{\Psi}_\kappa(\ell, \mathbf{t}_1; \lambda) &= \mathbf{S}^{-1} \left\{ \underline{\Psi}_\kappa(\ell, \mathbf{t}_1; \lambda) \right\} \\ &= \underline{\Psi}_0(\ell, \mathbf{t}_1; \lambda) + \underline{\Psi}_1(\ell, \mathbf{t}_1; \lambda) + \dots \end{aligned}$$

Repeating the same procedure for the upper case of (24). Therefore, we mention the solution in a parameterized version as follows:

$$\begin{cases} \underline{\Psi}(\ell, \mathbf{t}_1; \lambda) = \underline{\Psi}_0(\ell, \mathbf{t}_1; \lambda) + \underline{\Psi}_1(\ell, \mathbf{t}_1; \lambda) + \dots, \\ \bar{\Psi}(\ell, \mathbf{t}_1; \lambda) = \bar{\Psi}_0(\ell, \mathbf{t}_1; \lambda) + \bar{\Psi}_1(\ell, \mathbf{t}_1; \lambda) + \dots. \end{cases}$$

4. Convergence Analysis of Fuzzy SHPTM

Now, we describe the convergence analysis of the fuzzy SHPTM for the generalized fuzzy operator equation by employing the approach proposed by [57]:

$$\mathcal{L}(\tilde{\Psi}(\ell, \mathbf{t}_1; \lambda)) \oplus \mathcal{R}(\tilde{\Psi}(\ell, \mathbf{t}_1; \lambda)) \oplus \mathcal{N}(\tilde{\Psi}(\ell, \mathbf{t}_1; \lambda)) = \tilde{g}(\ell, \mathbf{t}_1; \lambda), \quad \lambda \in [0, 1], \quad (34)$$

where $\tilde{g}(\ell, \mathbf{t}_1; \lambda)$ is defined in \mathbb{H} . Suppose that there is an operator \mathbb{T} defined by $\mathbb{T}\tilde{\Psi}(\ell, \mathbf{t}_1; \lambda) = -\mathcal{R}\tilde{\Psi}(\ell, \mathbf{t}_1; \lambda) - \mathcal{N}\tilde{\Psi}(\ell, \mathbf{t}_1; \lambda)$.

Now, we assume that the Hilbert space $\mathbb{H} = \mathcal{L}^2((\gamma_1^*, \gamma_2^*) \times [0, \mathbb{T}])$ is presented by the following:

$$\tilde{\Psi}(\ell, \mathbf{t}_1; \lambda) : (\gamma_1^*, \gamma_2^*) \times [0, \mathbb{T}] \mapsto \mathbb{R}$$

along with:

$$\int_{(\gamma_1^*, \gamma_2^*) \times [0, \mathbb{T}]} \tilde{\Psi}(\ell, \mathbf{t}_1; \lambda) d\ell d\mathbf{t}_1 < +\infty,$$

where $\tilde{\Psi}(\ell, \mathbf{t}_1; \lambda) = [\underline{\Psi}(\ell, \mathbf{t}_1; \lambda), \bar{\Psi}(\ell, \mathbf{t}_1; \lambda)]$.

Theorem 2. Let there be a mapping $\mathbb{T}\tilde{\Psi}(\ell, \mathbf{t}_1; \lambda) = -\mathcal{R}\tilde{\Psi}(\ell, \mathbf{t}_1; \lambda) - \mathcal{N}\tilde{\Psi}(\ell, \mathbf{t}_1; \lambda)$ which is semi-continuous and holds the following assumptions:

(i): $(\mathbb{T}\tilde{\Psi}_1(\ell, \mathbf{t}_1; \lambda) - \mathbb{T}\tilde{\Psi}_2(\ell, \mathbf{t}_1; \lambda), \tilde{\Psi}_1(\ell, \mathbf{t}_1; \lambda) - \tilde{\Psi}_2(\ell, \mathbf{t}_1; \lambda)) \geq \mathcal{K}\|\tilde{\Psi}_1(\ell, \mathbf{t}_1; \lambda) - \tilde{\Psi}_2(\ell, \mathbf{t}_1; \lambda)\|^2, \mathcal{K} > 0, \forall \tilde{\Psi}_1, \tilde{\Psi}_2 \in \mathbb{H}$;

(ii): $\forall \mathcal{M} > 0, \exists D(\mathcal{M}) > 0$ such that for $\|\tilde{\Psi}_1\| \leq \mathcal{M}, \|\tilde{\Psi}_2\| \leq \mathcal{M}, \tilde{\Psi}_1, \tilde{\Psi}_2 \in \mathbb{H}$, we find:

$$\implies (\mathbb{T}\tilde{\Psi}_1(\ell, \mathbf{t}_1; \lambda) - \tilde{\Psi}_2(\ell, \mathbf{t}_1; \lambda), \tilde{w}(\ell, \mathbf{t}_1; \lambda)) \leq D(\mathcal{M})\|\tilde{\Psi}_1(\ell, \mathbf{t}_1; \lambda) - \tilde{\Psi}_1(\ell, \mathbf{t}_1; \lambda)\|^2\|\tilde{w}_1(\ell, \mathbf{t}_1; \lambda)\|^2, \quad \forall \tilde{w} \in \mathbb{H}.$$

For every $\tilde{g}(\ell, \mathbf{t}_1; \lambda) \in \mathbb{H}$, the general nonlinear fuzzy Equation (34) has a unique solution $\tilde{\Psi}(\ell, \mathbf{t}_1; \lambda) \in \mathbb{H}$. Furthermore, if the solution $\tilde{\Psi}(\ell, \mathbf{t}_1; \lambda)$ can be assimilated as a series $\tilde{\Psi}(\ell, \mathbf{t}_1; \lambda) = \sum_{\kappa=0}^{+\infty} \tilde{\Psi}_\kappa(\ell, \mathbf{t}_1; \lambda)\Xi^\kappa$, then the fuzzy SHPTM corresponding to the functional equation under investigation converges to $\tilde{\Psi}(\ell, \mathbf{t}_1; \lambda) \in \mathbb{H}$, which is the unique solution to the functional Equation (34).

For the sake of simplicity, the proof is followed by Osman et al. [58].

5. Functioning of the SHPTM and Mathematical Findings

Here, we elaborate the approximate-analytical solution of the fuzzy fractional Cauchy reaction–diffusion models via the Shehu homotopy perturbation transform method involving the CFD and ABC fractional derivative operators, respectively. Throughout this investigation, the MATLAB 2021 software package was considered for the graphical representation processes.

Problem 1. Assume the fuzzy time-fractional Cauchy-reaction diffusion model:

$$\frac{\partial^\vartheta}{\partial \mathbf{t}_1^\vartheta} \tilde{\Psi}(\ell, \mathbf{t}_1; \lambda) = \frac{\partial^2}{\partial \ell^2} \tilde{\Psi}(\ell, \mathbf{t}_1; \lambda) \ominus \tilde{\Psi}(\ell, \mathbf{t}_1; \lambda), \quad 0 < \vartheta \leq 1, \quad (35)$$

subject to fuzzy ICs:

$$\tilde{\Psi}(\ell, 0) = \tilde{Y}(\lambda) \odot (\exp(-\ell) \oplus \ell), \quad (36)$$

where: $\tilde{Y}(\lambda) = [\underline{Y}(\lambda), \bar{Y}(\lambda)] = [\lambda - 1, 1 - \lambda]$ for $\lambda \in [0, 1]$ is a fuzzy number.

The parameterized formulation of (35) is presented as

$$\begin{cases} \frac{\partial^\vartheta}{\partial \mathbf{t}_1^\vartheta} \underline{\Psi}(\ell, \mathbf{t}_1; \lambda) = \frac{\partial^2}{\partial \ell^2} \underline{\Psi}(\ell, \mathbf{t}_1; \lambda) - \underline{\Psi}(\ell, \mathbf{t}_1; \lambda), \\ \underline{\Psi}(\ell, 0) = (\lambda - 1)(\exp(-\ell) + \ell) \\ \frac{\partial^\vartheta}{\partial \mathbf{t}_1^\vartheta} \bar{\Psi}(\ell, \mathbf{t}_1; \lambda) = \frac{\partial^2}{\partial \ell^2} \bar{\Psi}(\ell, \mathbf{t}_1; \lambda) - \bar{\Psi}(\ell, \mathbf{t}_1; \lambda), \\ \bar{\Psi}(\ell, 0) = (1 - \lambda)(\exp(-\ell) + \ell). \end{cases}$$

Case 1. Firstly, take into consideration the CFD coupled with the Shehu homotopy perturbation transform method in the first case of (37).

Considering the process stated in Section 3, we have:

$$\left(\frac{\nu}{\xi}\right)^\vartheta \mathbf{S}[\underline{\Psi}(\ell, \mathbf{t}_1; \lambda)] - \sum_{\kappa=0}^{r-1} \left(\frac{\xi}{\nu}\right)^{\vartheta-\kappa-1} \underline{\Psi}^{(\kappa)}(0) = \mathbf{S} \left[\frac{\partial^2}{\partial \ell^2} \underline{\Psi}(\ell, \mathbf{t}_1; \lambda) - \underline{\Psi}(\ell, \mathbf{t}_1; \lambda) \right].$$

Considering the fuzzy IC, making use of the inverse Shehu transform implies that:

$$\underline{\Psi}(\ell, \mathbf{t}_1; \lambda) = \frac{\nu}{\xi}(\lambda - 1)(\ell + \exp(-\ell)) + \mathbf{S}^{-1} \left[\left(\frac{\nu}{\xi}\right)^\vartheta \mathbf{S} \left[\frac{\partial^2}{\partial \ell^2} \underline{\Psi}(\ell, \mathbf{t}_1; \lambda) - \underline{\Psi}(\ell, \mathbf{t}_1; \lambda) \right] \right].$$

Now implementing the HPM, we have:

$$\begin{aligned} \sum_{\kappa=0}^{+\infty} \eta^\kappa \underline{\Psi}_\kappa(\ell, \mathbf{t}_1; \lambda) &= (\lambda - 1)(\ell + \exp(-\ell)) \\ &+ \eta \left(\mathbf{S}^{-1} \left[\left(\frac{\nu}{\xi}\right)^\vartheta \mathbf{S} \left[\left(\sum_{\kappa=0}^{+\infty} \eta^\kappa \underline{\Psi}_\kappa(\ell, \mathbf{t}_1; \lambda) \right)_{\ell\ell} - \left(\sum_{\kappa=0}^{+\infty} \eta^\kappa \underline{\Psi}_\kappa(\ell, \mathbf{t}_1; \lambda) \right) \right] \right] \right). \end{aligned}$$

Equating the coefficients of the same powers of η , we have:

$$\begin{aligned} \eta^0 : \underline{\Psi}_0(\ell, \mathbf{t}_1; \lambda) &= (\lambda - 1)(\ell + \exp(-\ell)), \\ \eta^1 : \underline{\Psi}_1(\ell, \mathbf{t}_1; \lambda) &= \mathbf{S}^{-1} \left[\left(\frac{\nu}{\xi}\right)^\vartheta \mathbf{S} \left[(\underline{\Psi}_0(\ell, \mathbf{t}_1; \lambda))_{\ell\ell} - \underline{\Psi}_0(\ell, \mathbf{t}_1; \lambda) \right] \right] = -(\lambda - 1)\ell \frac{\mathbf{t}_1^\vartheta}{\Gamma(\vartheta + 1)}, \\ \eta^2 : \underline{\Psi}_1(\ell, \mathbf{t}_1; \lambda) &= \mathbf{S}^{-1} \left[\left(\frac{\nu}{\xi}\right)^\vartheta \mathbf{S} \left[(\underline{\Psi}_1(\ell, \mathbf{t}_1; \lambda))_{\ell\ell} - \underline{\Psi}_1(\ell, \mathbf{t}_1; \lambda) \right] \right] = (\lambda - 1)\ell \frac{\mathbf{t}_1^{2\vartheta}}{\Gamma(2\vartheta + 1)}, \\ \eta^3 : \underline{\Psi}_2(\ell, \mathbf{t}_1; \lambda) &= \mathbf{S}^{-1} \left[\left(\frac{\nu}{\xi}\right)^\vartheta \mathbf{S} \left[(\underline{\Psi}_2(\ell, \mathbf{t}_1; \lambda))_{\ell\ell} - \underline{\Psi}_2(\ell, \mathbf{t}_1; \lambda) \right] \right] = -(\lambda - 1)\ell \frac{\mathbf{t}_1^{3\vartheta}}{\Gamma(3\vartheta + 1)}, \\ &\vdots \end{aligned}$$

The series form solution is presented as follows:

$$\tilde{\Psi}(\ell, \mathbf{t}_1; \lambda) = \tilde{\Psi}_0(\ell, \mathbf{t}_1; \lambda) + \tilde{\Psi}_1(\ell, \mathbf{t}_1; \lambda) + \tilde{\Psi}_2(\ell, \mathbf{t}_1; \lambda) + \tilde{\Psi}_3(\ell, \mathbf{t}_1; \lambda) + \dots,$$

which implies that:

$$\begin{aligned} \underline{\Psi}(\ell, \mathbf{t}_1; \lambda) &= \underline{\Psi}_0(\ell, \mathbf{t}_1; \lambda) + \underline{\Psi}_1(\ell, \mathbf{t}_1; \lambda) + \underline{\Psi}_2(\ell, \mathbf{t}_1; \lambda) + \underline{\Psi}_3(\ell, \mathbf{t}_1; \lambda) + \dots, \\ \bar{\Psi}(\ell, \mathbf{t}_1; \lambda) &= \bar{\Psi}_0(\ell, \mathbf{t}_1; \lambda) + \bar{\Psi}_1(\ell, \mathbf{t}_1; \lambda) + \bar{\Psi}_2(\ell, \mathbf{t}_1; \lambda) + \bar{\Psi}_3(\ell, \mathbf{t}_1; \lambda) + \dots \end{aligned}$$

Finally, we have:

$$\begin{aligned}\underline{\Psi}(\ell, \mathbf{t}_1; \lambda) &= (\lambda - 1) \exp(-\ell) + (\lambda - 1) \ell \left[1 - \frac{\mathbf{t}_1^\vartheta}{\Gamma(\vartheta + 1)} + \frac{\mathbf{t}_1^{2\vartheta}}{\Gamma(2\vartheta + 1)} - \frac{\mathbf{t}_1^{3\vartheta}}{\Gamma(3\vartheta + 1)} + \dots \right], \\ \tilde{\Psi}(\ell, \mathbf{t}_1; \lambda) &= (1 - \lambda) \exp(-\ell) + (1 - \lambda) \ell \left[1 - \frac{\mathbf{t}_1^\vartheta}{\Gamma(\vartheta + 1)} + \frac{\mathbf{t}_1^{2\vartheta}}{\Gamma(2\vartheta + 1)} - \frac{\mathbf{t}_1^{3\vartheta}}{\Gamma(3\vartheta + 1)} + \dots \right].\end{aligned}$$

Case 2. Now, we employ the fuzzy ABC derivative operator in the first case of (37) as follows.

Considering the process stated in Section 3, we have:

$$\frac{\mathbb{B}(\vartheta)}{1 - \vartheta + \vartheta \left(\frac{\nu}{\xi}\right)^\vartheta} \mathbf{S}[\underline{\Psi}(\ell, \mathbf{t}_1; \lambda)] - \frac{\mathbb{B}(\vartheta)}{1 - \vartheta + \vartheta \left(\frac{\nu}{\xi}\right)^\vartheta} \left(\frac{\nu}{\xi}\right)^\vartheta \underline{\Psi}(\ell, 0) = \mathbf{S} \left[\frac{\partial^2}{\partial \ell^2} \underline{\Psi}(\ell, \mathbf{t}_1; \lambda) - \underline{\Psi}(\ell, \mathbf{t}_1; \lambda) \right].$$

Considering the fuzzy IC, making use of the inverse Shehu transform implies that:

$$\underline{\Psi}(\ell, \mathbf{t}_1; \lambda) = \frac{\nu}{\xi} (\lambda - 1) (\ell + \exp(-\ell)) + \mathbf{S}^{-1} \left[\frac{1 - \vartheta + \vartheta \left(\frac{\nu}{\xi}\right)^\vartheta}{\mathbb{B}(\vartheta)} \mathbf{S} \left[\frac{\partial^2}{\partial \ell^2} \underline{\Psi}(\ell, \mathbf{t}_1; \lambda) - \underline{\Psi}(\ell, \mathbf{t}_1; \lambda) \right] \right].$$

Now, by implementing the HPM, we have:

$$\begin{aligned}\sum_{\kappa=0}^{+\infty} \eta^\kappa \underline{\Psi}_\kappa(\ell, \mathbf{t}_1; \lambda) &= (\lambda - 1) (\ell + \exp(-\ell)) \\ &+ \eta \left(\mathbf{S}^{-1} \left[\frac{1 - \vartheta + \vartheta \left(\frac{\nu}{\xi}\right)^\vartheta}{\mathbb{B}(\vartheta)} \mathbf{S} \left[\left(\sum_{\kappa=0}^{+\infty} \eta^\kappa \underline{\Psi}_\kappa(\ell, \mathbf{t}_1; \lambda) \right)_{\ell\ell} - \left(\sum_{\kappa=0}^{+\infty} \eta^\kappa \underline{\Psi}_\kappa(\ell, \mathbf{t}_1; \lambda) \right) \right] \right] \right).\end{aligned}$$

By equating the coefficients of the same powers of η , we have:

$$\begin{aligned}\eta^0 : \underline{\Psi}_0(\ell, \mathbf{t}_1; \lambda) &= (\lambda - 1) (\ell + \exp(-\ell)), \\ \eta^1 : \underline{\Psi}_1(\ell, \mathbf{t}_1; \lambda) &= \mathbf{S}^{-1} \left[\frac{1 - \vartheta + \vartheta \left(\frac{\nu}{\xi}\right)^\vartheta}{\mathbb{B}(\vartheta)} \mathbf{S} \left[(\underline{\Psi}_0(\ell, \mathbf{t}_1; \lambda))_{\ell\ell} - \underline{\Psi}_0(\ell, \mathbf{t}_1; \lambda) \right] \right] \\ &= -\frac{(\lambda - 1) \ell}{\mathbb{B}(\vartheta)} \left[\frac{\vartheta \mathbf{t}_1^\vartheta}{\Gamma(\vartheta + 1)} + (1 - \vartheta) \right], \\ \eta^2 : \underline{\Psi}_2(\ell, \mathbf{t}_1; \lambda) &= \mathbf{S}^{-1} \left[\frac{1 - \vartheta + \vartheta \left(\frac{\nu}{\xi}\right)^\vartheta}{\mathbb{B}(\vartheta)} \mathbf{S} \left[(\underline{\Psi}_1(\ell, \mathbf{t}_1; \lambda))_{\ell\ell} - \underline{\Psi}_1(\ell, \mathbf{t}_1; \lambda) \right] \right] \\ &= \frac{(\lambda - 1) \ell}{\mathbb{B}^2(\vartheta)} \left[\frac{\vartheta^2 \mathbf{t}_1^{2\vartheta}}{\Gamma(2\vartheta + 1)} + 2\vartheta(1 - \vartheta) \frac{\mathbf{t}_1^\vartheta}{\Gamma(\vartheta + 1)} + (1 - \vartheta)^2 \right], \\ \eta^3 : \underline{\Psi}_3(\ell, \mathbf{t}_1; \lambda) &= \mathbf{S}^{-1} \left[\frac{1 - \vartheta + \vartheta \left(\frac{\nu}{\xi}\right)^\vartheta}{\mathbb{B}(\vartheta)} \mathbf{S} \left[(\underline{\Psi}_2(\ell, \mathbf{t}_1; \lambda))_{\ell\ell} - \underline{\Psi}_2(\ell, \mathbf{t}_1; \lambda) \right] \right] \\ &= -\frac{(\lambda - 1) \ell}{\mathbb{B}^3(\vartheta)} \left[\frac{\vartheta^3 \mathbf{t}_1^{3\vartheta}}{\Gamma(3\vartheta + 1)} + 3\vartheta^2(1 - \vartheta) \frac{\mathbf{t}_1^{2\vartheta}}{\Gamma(2\vartheta + 1)} + 3\vartheta(1 - \vartheta)^2 \frac{\mathbf{t}_1^\vartheta}{\Gamma(\vartheta + 1)} + (1 - \vartheta)^3 \right], \\ &\vdots\end{aligned}$$

The series form solution is presented as follows:

$$\tilde{\Psi}(\ell, \mathbf{t}_1; \lambda) = \tilde{\Psi}_0(\ell, \mathbf{t}_1; \lambda) + \tilde{\Psi}_1(\ell, \mathbf{t}_1; \lambda) + \tilde{\Psi}_2(\ell, \mathbf{t}_1; \lambda) + \tilde{\Psi}_3(\ell, \mathbf{t}_1; \lambda) + \dots,$$

which implies that:

$$\begin{aligned}\underline{\Psi}(\ell, \mathbf{t}_1; \lambda) &= \underline{\Psi}_0(\ell, \mathbf{t}_1; \lambda) + \underline{\Psi}_1(\ell, \mathbf{t}_1; \lambda) + \underline{\Psi}_2(\ell, \mathbf{t}_1; \lambda) + \underline{\Psi}_3(\ell, \mathbf{t}_1; \lambda) + \dots, \\ \bar{\Psi}(\ell, \mathbf{t}_1; \lambda) &= \bar{\Psi}_0(\ell, \mathbf{t}_1; \lambda) + \bar{\Psi}_1(\ell, \mathbf{t}_1; \lambda) + \bar{\Psi}_2(\ell, \mathbf{t}_1; \lambda) + \bar{\Psi}_3(\ell, \mathbf{t}_1; \lambda) + \dots.\end{aligned}$$

Finally, we have:

$$\begin{aligned}\underline{\Psi}(\ell, \mathbf{t}_1; \lambda) &= (\lambda - 1) \exp(-\ell) + (\lambda - 1) \ell \left\{ \begin{aligned} &1 - \frac{1}{\mathbb{B}(\vartheta)} \left[\frac{\vartheta \mathbf{t}_1^\vartheta}{\Gamma(\vartheta+1)} + (1 - \vartheta) \right] \\ &+ \frac{1}{\mathbb{B}^2(\vartheta)} \left[\frac{\vartheta^2 \mathbf{t}_1^{2\vartheta}}{\Gamma(2\vartheta+1)} + 2\vartheta(1 - \vartheta) \frac{\mathbf{t}_1^\vartheta}{\Gamma(\vartheta+1)} + (1 - \vartheta)^2 \right] \\ &- \frac{1}{\mathbb{B}^3(\vartheta)} \left[\frac{\vartheta^3 \mathbf{t}_1^{3\vartheta}}{\Gamma(3\vartheta+1)} + 3\vartheta^2(1 - \vartheta) \frac{\mathbf{t}_1^{2\vartheta}}{\Gamma(2\vartheta+1)} + 3\vartheta(1 - \vartheta)^2 \frac{\mathbf{t}_1^\vartheta}{\Gamma(\vartheta+1)} + (1 - \vartheta)^3 \right] + \dots, \end{aligned} \right. \\ \bar{\Psi}(\ell, \mathbf{t}_1; \lambda) &= (1 - \lambda) \exp(-\ell) + (1 - \lambda) \ell \left\{ \begin{aligned} &1 - \frac{1}{\mathbb{B}(\vartheta)} \left[\frac{\vartheta \mathbf{t}_1^\vartheta}{\Gamma(\vartheta+1)} + (1 - \vartheta) \right] \\ &+ \frac{1}{\mathbb{B}^2(\vartheta)} \left[\frac{\vartheta^2 \mathbf{t}_1^{2\vartheta}}{\Gamma(2\vartheta+1)} + 2\vartheta(1 - \vartheta) \frac{\mathbf{t}_1^\vartheta}{\Gamma(\vartheta+1)} + (1 - \vartheta)^2 \right] \\ &- \frac{1}{\mathbb{B}^3(\vartheta)} \left[\frac{\vartheta^3 \mathbf{t}_1^{3\vartheta}}{\Gamma(3\vartheta+1)} + 3\vartheta^2(1 - \vartheta) \frac{\mathbf{t}_1^{2\vartheta}}{\Gamma(2\vartheta+1)} + 3\vartheta(1 - \vartheta)^2 \frac{\mathbf{t}_1^\vartheta}{\Gamma(\vartheta+1)} + (1 - \vartheta)^3 \right] + \dots. \end{aligned} \right.\end{aligned}\tag{37}$$

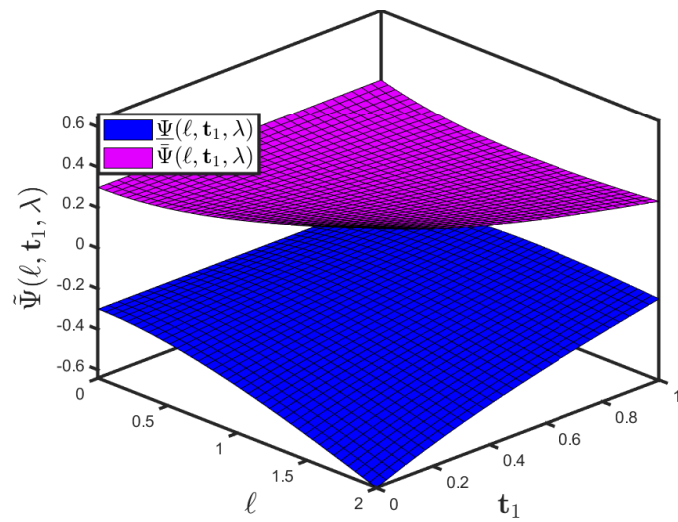
Figure 1a,b reveal how the effectiveness of multiple (lower and upper bound accuracy) surface graphs for Problem 2 interacting with the fuzzy CFD and Shehu transform is being exhibited in this investigation. The pattern specifies the fluctuation in the mapping $\bar{\Psi}(\ell, \mathbf{t}_1; \lambda)$ on the space co-ordinate ℓ with the consideration of \mathbf{t}_1 and the uncertainty parameter $\lambda \in [0, 1]$. The figure illustrates that, as time passes, the mapping $\bar{\Psi}(\ell, \mathbf{t}_1; \lambda)$ will become more intricate.

Figure 2a highlights the impact of the suggested technique on the mapping $\bar{\Psi}(\ell, \mathbf{t}_1; \lambda)$ for the fuzzy CFD to have an uncertainty parameter $\lambda \in [0, 1]$. With the slight increase in $\bar{\Psi}(\ell, \mathbf{t}_1; \lambda)$, it then clearly demonstrates a large decrease in the mapping $\underline{\Psi}(\ell, \mathbf{t}_1; \lambda)$. Figure 2b highlights the effect of the recommended approach on the mapping $\bar{\Psi}(\ell, \mathbf{t}_1; \lambda)$ for the fuzzy CFD to have a fixed fractional order with the varying uncertainty parameter $\lambda \in [0, 1]$. With a small increase in the uncertainty parameter, the mappings $\bar{\Psi}(\ell, \mathbf{t}_1; \lambda)$ and $\underline{\Psi}(\ell, \mathbf{t}_1; \lambda)$ are stable.

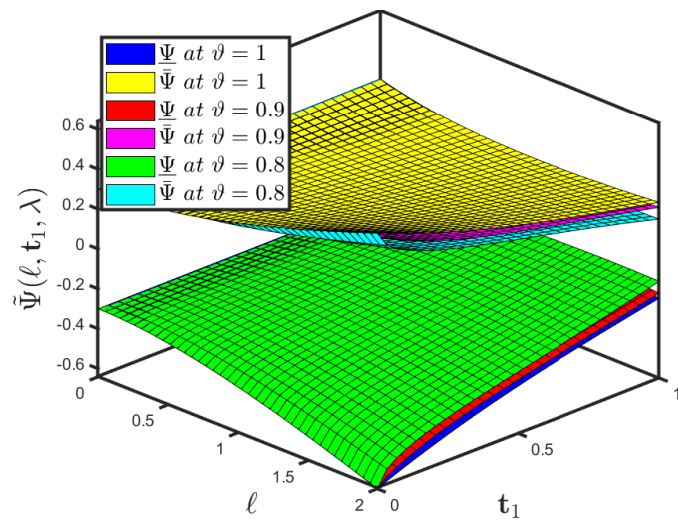
Figure 3a highlights the impact of the suggested technique on the mapping $\bar{\Psi}(\ell, \mathbf{t}_1; \lambda)$ for the fuzzy ABC to have an uncertainty parameter $\lambda \in [0, 1]$. With the slight increase in $\bar{\Psi}(\ell, \mathbf{t}_1; \lambda)$, it then clearly demonstrates a large decrease in the mapping $\underline{\Psi}(\ell, \mathbf{t}_1; \lambda)$. Figure 3b highlights the effect of the recommended approach on the mapping $\bar{\Psi}(\ell, \mathbf{t}_1; \lambda)$ for the fuzzy ABC to have a fixed fractional order with the varying uncertainty parameter $\lambda \in [0, 1]$. With a small increase in the uncertainty parameter, the mappings $\bar{\Psi}(\ell, \mathbf{t}_1; \lambda)$ and $\underline{\Psi}(\ell, \mathbf{t}_1; \lambda)$ are stable.

Figure 4a,b illustrate the comparison between the lower and upper bound accuracies for fuzzy CFD and fuzzy ABC fractional derivative operators for Problem 1 established by the SHPTM for standard motion, i.e., at $\vartheta = 1$.

The graphs in Figures 1–4 assist in recognizing how time and space variation statistically interact. In addition, the proposed method will facilitate scientists' work on pattern formation, diffusion, instability theory, and monitoring competence by employing inferential statistical testing.

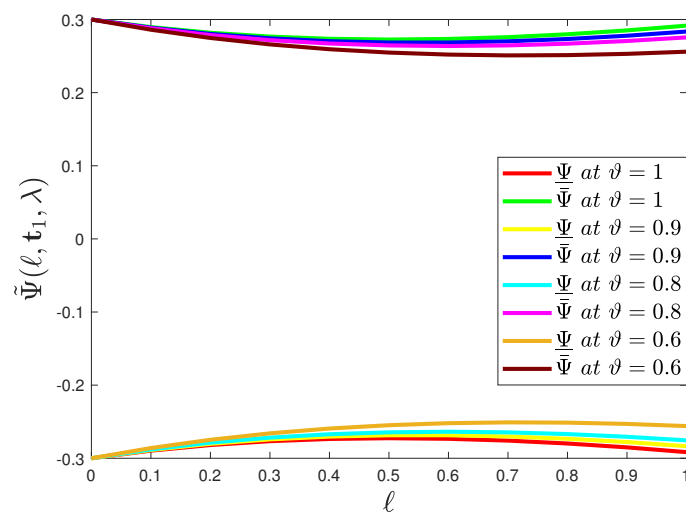


(a)

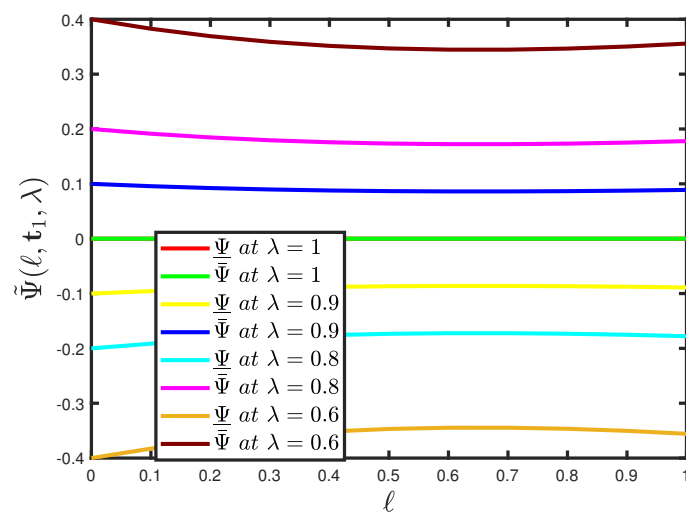


(b)

Figure 1. Three-dimensional plot of $\tilde{\Psi}(\ell, t_1; \lambda)$ of Problem (1): (a) $\Psi(\ell, t_1; \lambda)$ and $\bar{\Psi}(\ell, t_1; \lambda)$ when $\vartheta = 1$; and (b) $\Psi(\ell, t_1; \lambda)$ and $\bar{\Psi}(\ell, t_1; \lambda)$ when the uncertainty parameter $\lambda \in [0, 1]$ has different fractional orders.

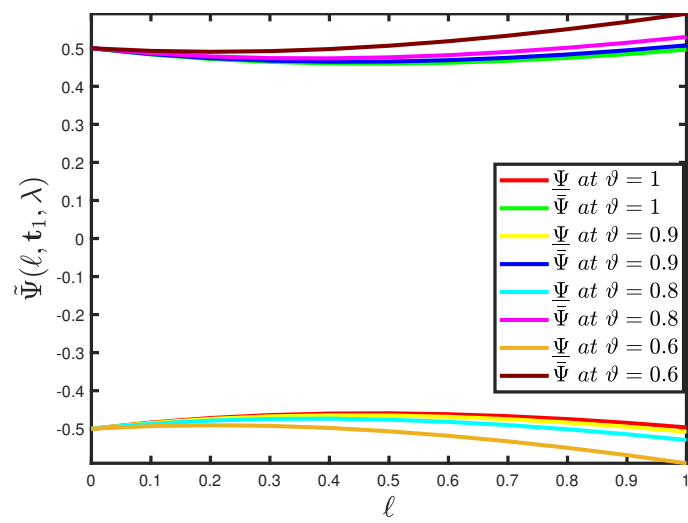


(a)

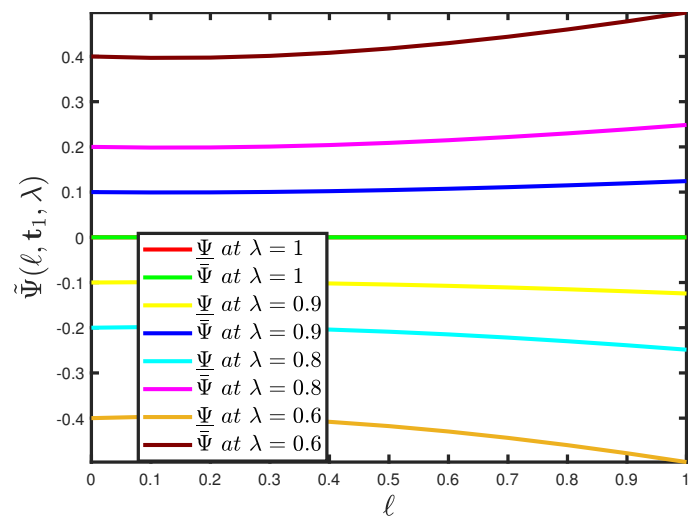


(b)

Figure 2. Two-dimensional simulation of $\tilde{\Psi}(\ell, \mathbf{t}_1; \lambda)$ of Problem (1): (a) $\underline{\Psi}(\ell, \mathbf{t}_1; \lambda)$ and $\tilde{\Psi}(\ell, \mathbf{t}_1; \lambda)$ when fuzzy CFD is considered to have an uncertainty parameter $\lambda \in [0, 1]$ and $\mathbf{t}_1 = 0.7$; and (b) $\underline{\Psi}(\ell, \mathbf{t}_1; \lambda)$ and $\tilde{\Psi}(\ell, \mathbf{t}_1; \lambda)$ when fuzzy CFD is considered to have a fractional order $\vartheta = 0.7$ and $\mathbf{t}_1 = 0.7$.



(a)



(b)

Figure 3. Two-dimensional simulation of $\tilde{\Psi}(\ell, \mathbf{t}_1; \lambda)$ of Problem (1): (a) $\underline{\Psi}(\ell, \mathbf{t}_1; \lambda)$ and $\tilde{\Psi}(\ell, \mathbf{t}_1; \lambda)$ when fuzzy ABC is considered to have an uncertainty parameter $\lambda \in [0, 1]$ and $\mathbf{t}_1 = 0.7$; and (b) $\underline{\Psi}(\ell, \mathbf{t}_1; \lambda)$ and $\tilde{\Psi}(\ell, \mathbf{t}_1; \lambda)$ when fuzzy ABC is considered to have a fractional order $\vartheta = 0.7$ and $\mathbf{t}_1 = 0.7$.

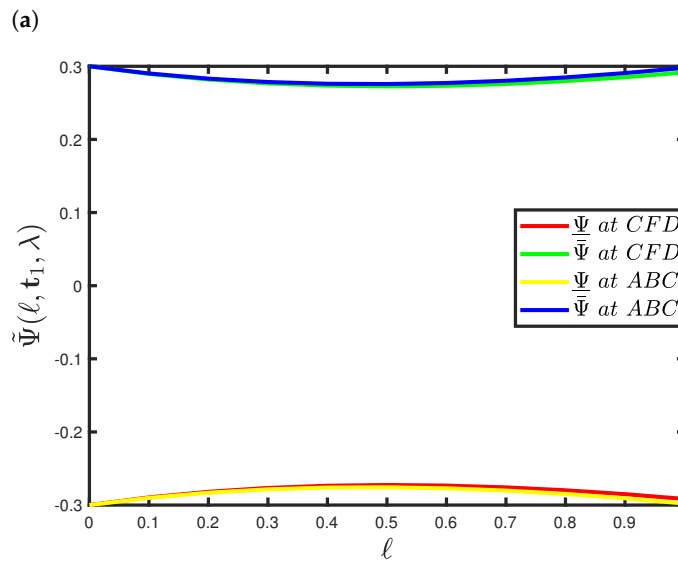
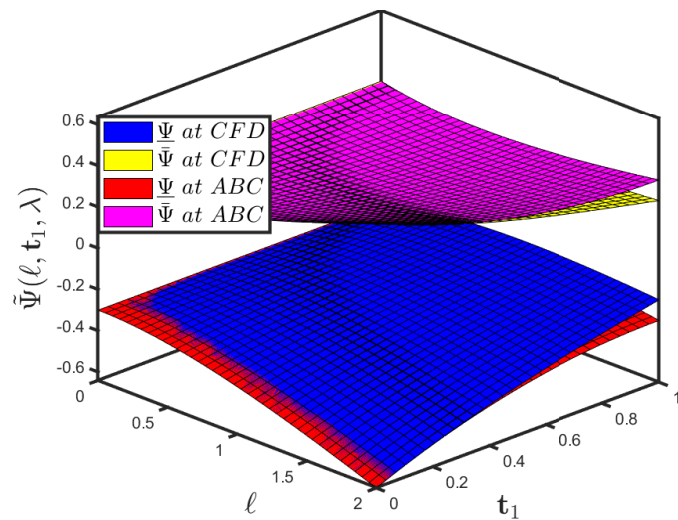


Figure 4. Comparison plots of $\tilde{\Psi}(\ell, t_1; \lambda)$ of Problem (1) when fuzzy CFD and ABC are considered to have a fractional order $\vartheta = 1$ and uncertainty parameter $\lambda \in [0, 1]$: (a) three-dimensional plot; and (b) two-dimensional plot of $\underline{\Psi}(\ell, t_1; \lambda)$, $\bar{\Psi}(\ell, t_1; \lambda)$ and $t_1 = 0.7$.

Remark 2. When $[\lambda - 1, 1 - \lambda] = 1$ and $\vartheta = 1$, then solution (37) reduces to the integer-order solution $\Psi(\ell, t_1) = \exp(-\ell) + \ell \exp(t_1)$.

Problem 2. Assume that the fuzzy time-fractional Cauchy-reaction diffusion model:

$$\frac{\partial^\vartheta}{\partial t_1^\vartheta} \tilde{\Psi}(\ell, t_1; \lambda) = \frac{\partial^2}{\partial \ell^2} \tilde{\Psi}(\ell, t_1; \lambda) \ominus (1 \oplus 4 \odot \ell^2) \tilde{\Psi}(\ell, t_1; \lambda), \quad 0 < \vartheta \leq 1, \tag{38}$$

is subject to the fuzzy initial condition:

$$\tilde{\Psi}(\ell, 0) = \tilde{Y}(\lambda) \odot \exp(\ell^2), \tag{39}$$

where $\tilde{Y}(\lambda) = [\underline{Y}(\lambda), \bar{Y}(\lambda)] = [\lambda - 1, 1 - \lambda]$ for $\lambda \in [0, 1]$ is the fuzzy number.

The parameterized formulation of (35) is presented as

$$\begin{cases} \frac{\partial^\vartheta}{\partial \mathbf{t}_1^\vartheta} \underline{\Psi}(\ell, \mathbf{t}_1; \lambda) = \frac{\partial^2}{\partial \ell^2} \underline{\Psi}(\ell, \mathbf{t}_1; \lambda) - (1 + 4\ell^2) \underline{\Psi}(\ell, \mathbf{t}_1; \lambda), \\ \underline{\Psi}(\ell, 0) = (\lambda - 1) \exp(\ell^2) \\ \frac{\partial^\vartheta}{\partial \mathbf{t}_1^\vartheta} \bar{\Psi}(\ell, \mathbf{t}_1; \lambda) = \frac{\partial^2}{\partial \ell^2} \bar{\Psi}(\ell, \mathbf{t}_1; \lambda) - (1 + 4\ell^2) \bar{\Psi}(\ell, \mathbf{t}_1; \lambda), \\ \bar{\Psi}(\ell, 0) = (1 - \lambda) \exp(\ell^2). \end{cases}$$

Case 1. Firstly, we take into consideration the fuzzy CFD coupled with the Shehu homotopy perturbation transform method in the first case of (40).

Considering the process stated in Section 3, we have:

$$\left(\frac{\nu}{\xi}\right)^\vartheta \mathbf{S}[\underline{\Psi}(\ell, \mathbf{t}_1; \lambda)] - \sum_{\kappa=0}^{r-1} \left(\frac{\xi}{\nu}\right)^{\vartheta-\kappa-1} \underline{\Psi}^{(\kappa)}(0) = \mathbf{S} \left[\frac{\partial^2}{\partial \ell^2} \underline{\Psi}(\ell, \mathbf{t}_1; \lambda) - (1 + 4\ell^2) \underline{\Psi}(\ell, \mathbf{t}_1; \lambda) \right].$$

Considering the fuzzy IC, making use of the inverse Shehu transform implies that:

$$\underline{\Psi}(\ell, \mathbf{t}_1; \lambda) = \frac{\nu}{\xi} (\lambda - 1) \exp(\ell^2) + \mathbf{S}^{-1} \left[\left(\frac{\nu}{\xi}\right)^\vartheta \mathbf{S} \left[\frac{\partial^2}{\partial \ell^2} \underline{\Psi}(\ell, \mathbf{t}_1; \lambda) - (1 + 4\ell^2) \underline{\Psi}(\ell, \mathbf{t}_1; \lambda) \right] \right].$$

Now, by implementing the HPM, we have:

$$\sum_{\kappa=0}^{+\infty} \eta^\kappa \underline{\Psi}_\kappa(\ell, \mathbf{t}_1; \lambda) = (\lambda - 1) \exp(\ell^2) + \eta \left(\mathbf{S}^{-1} \left[\left(\frac{\nu}{\xi}\right)^\vartheta \mathbf{S} \left[\left(\sum_{\kappa=0}^{+\infty} \eta^\kappa \underline{\Psi}_\kappa(\ell, \mathbf{t}_1; \lambda) \right)_{\ell\ell} - (1 + 4\ell^2) \left(\sum_{\kappa=0}^{+\infty} \eta^\kappa \underline{\Psi}_\kappa(\ell, \mathbf{t}_1; \lambda) \right) \right] \right] \right).$$

Equating the coefficients of the same powers of η , we have:

$$\begin{aligned} \eta^0 : \underline{\Psi}_0(\ell, \mathbf{t}_1; \lambda) &= (\lambda - 1) \exp(\ell^2), \\ \eta^1 : \underline{\Psi}_1(\ell, \mathbf{t}_1; \lambda) &= \mathbf{S}^{-1} \left[\left(\frac{\nu}{\xi}\right)^\vartheta \mathbf{S} \left[(\underline{\Psi}_0(\ell, \mathbf{t}_1; \lambda))_{\ell\ell} - (1 + 4\ell^2) \underline{\Psi}_0(\ell, \mathbf{t}_1; \lambda) \right] \right] = (\lambda - 1) \exp(\ell^2) \frac{\mathbf{t}_1^\vartheta}{\Gamma(\vartheta + 1)}, \\ \eta^2 : \underline{\Psi}_1(\ell, \mathbf{t}_1; \lambda) &= \mathbf{S}^{-1} \left[\left(\frac{\nu}{\xi}\right)^\vartheta \mathbf{S} \left[(\underline{\Psi}_1(\ell, \mathbf{t}_1; \lambda))_{\ell\ell} - (1 + 4\ell^2) \underline{\Psi}_1(\ell, \mathbf{t}_1; \lambda) \right] \right] = (\lambda - 1) \exp(\ell^2) \frac{\mathbf{t}_1^{2\vartheta}}{\Gamma(2\vartheta + 1)}, \\ \eta^3 : \underline{\Psi}_2(\ell, \mathbf{t}_1; \lambda) &= \mathbf{S}^{-1} \left[\left(\frac{\nu}{\xi}\right)^\vartheta \mathbf{S} \left[(\underline{\Psi}_2(\ell, \mathbf{t}_1; \lambda))_{\ell\ell} - (1 + 4\ell^2) \underline{\Psi}_2(\ell, \mathbf{t}_1; \lambda) \right] \right] = (\lambda - 1) \exp(\ell^2) \frac{\mathbf{t}_1^{3\vartheta}}{\Gamma(3\vartheta + 1)}, \\ &\vdots \end{aligned}$$

The series form solution is presented as follows:

$$\tilde{\Psi}(\ell, \mathbf{t}_1; \lambda) = \tilde{\Psi}_0(\ell, \mathbf{t}_1; \lambda) + \tilde{\Psi}_1(\ell, \mathbf{t}_1; \lambda) + \tilde{\Psi}_2(\ell, \mathbf{t}_1; \lambda) + \tilde{\Psi}_3(\ell, \mathbf{t}_1; \lambda) + \dots,$$

which implies that:

$$\begin{aligned} \underline{\Psi}(\ell, \mathbf{t}_1; \lambda) &= \underline{\Psi}_0(\ell, \mathbf{t}_1; \lambda) + \underline{\Psi}_1(\ell, \mathbf{t}_1; \lambda) + \underline{\Psi}_2(\ell, \mathbf{t}_1; \lambda) + \underline{\Psi}_3(\ell, \mathbf{t}_1; \lambda) + \dots, \\ \bar{\Psi}(\ell, \mathbf{t}_1; \lambda) &= \bar{\Psi}_0(\ell, \mathbf{t}_1; \lambda) + \bar{\Psi}_1(\ell, \mathbf{t}_1; \lambda) + \bar{\Psi}_2(\ell, \mathbf{t}_1; \lambda) + \bar{\Psi}_3(\ell, \mathbf{t}_1; \lambda) + \dots. \end{aligned}$$

Finally, we have:

$$\begin{aligned} \underline{\Psi}(\ell, \mathbf{t}_1; \lambda) &= (\lambda - 1) \exp(\ell^2) \left[1 - \frac{\mathbf{t}_1^\vartheta}{\Gamma(\vartheta + 1)} + \frac{\mathbf{t}_1^{2\vartheta}}{\Gamma(2\vartheta + 1)} - \frac{\mathbf{t}_1^{3\vartheta}}{\Gamma(3\vartheta + 1)} + \dots \right], \\ \bar{\Psi}(\ell, \mathbf{t}_1; \lambda) &= (1 - \lambda) \exp(\ell^2) \left[1 - \frac{\mathbf{t}_1^\vartheta}{\Gamma(\vartheta + 1)} + \frac{\mathbf{t}_1^{2\vartheta}}{\Gamma(2\vartheta + 1)} - \frac{\mathbf{t}_1^{3\vartheta}}{\Gamma(3\vartheta + 1)} + \dots \right]. \end{aligned}$$

Case 2. Now, we employ the fuzzy ABC derivative operator in the first case of (37) as follows.

Considering the process stated in Section 3, we have:

$$\frac{\mathbb{B}(\vartheta)}{1 - \vartheta + \vartheta\left(\frac{\nu}{\xi}\right)^\vartheta} \mathbf{S}[\underline{\Psi}(\ell, \mathbf{t}_1; \lambda)] - \frac{\mathbb{B}(\vartheta)}{1 - \vartheta + \vartheta\left(\frac{\nu}{\xi}\right)^\vartheta} \left(\frac{\nu}{\xi}\right)^\vartheta \underline{\Psi}(\ell, 0) = \mathbf{S} \left[\frac{\partial^2}{\partial \ell^2} \underline{\Psi}(\ell, \mathbf{t}_1; \lambda) - (1 + 4\ell^2) \underline{\Psi}(\ell, \mathbf{t}_1; \lambda) \right].$$

Considering the fuzzy initial condition, making use of the inverse Shehu transform implies that:

$$\underline{\Psi}(\ell, \mathbf{t}_1; \lambda) = \frac{\nu}{\xi} (\lambda - 1) \exp(\ell^2) + \mathbf{S}^{-1} \left[\frac{1 - \vartheta + \vartheta\left(\frac{\nu}{\xi}\right)^\vartheta}{\mathbb{B}(\vartheta)} \mathbf{S} \left[\frac{\partial^2}{\partial \ell^2} \underline{\Psi}(\ell, \mathbf{t}_1; \lambda) - (1 + 4\ell^2) \underline{\Psi}(\ell, \mathbf{t}_1; \lambda) \right] \right].$$

Now, by implementing the HPM, we have:

$$\begin{aligned} \sum_{\kappa=0}^{+\infty} \eta^\kappa \underline{\Psi}_\kappa(\ell, \mathbf{t}_1; \lambda) &= (\lambda - 1) \exp(\ell^2) \\ &+ \eta \left(\mathbf{S}^{-1} \left[\frac{1 - \vartheta + \vartheta\left(\frac{\nu}{\xi}\right)^\vartheta}{\mathbb{B}(\vartheta)} \mathbf{S} \left[\left(\sum_{\kappa=0}^{+\infty} \eta^\kappa \underline{\Psi}_\kappa(\ell, \mathbf{t}_1; \lambda) \right)_{\ell\ell} - (1 + 4\ell^2) \left(\sum_{\kappa=0}^{+\infty} \eta^\kappa \underline{\Psi}_\kappa(\ell, \mathbf{t}_1; \lambda) \right) \right] \right] \right). \end{aligned}$$

Equating the coefficients of the same powers of η , we have:

$$\begin{aligned} \eta^0 : \underline{\Psi}_0(\ell, \mathbf{t}_1; \lambda) &= (\lambda - 1) \exp(\ell^2), \\ \eta^1 : \underline{\Psi}_1(\ell, \mathbf{t}_1; \lambda) &= \mathbf{S}^{-1} \left[\frac{1 - \vartheta + \vartheta\left(\frac{\nu}{\xi}\right)^\vartheta}{\mathbb{B}(\vartheta)} \mathbf{S} \left[(\underline{\Psi}_0(\ell, \mathbf{t}_1; \lambda))_{\ell\ell} - (1 + 4\ell^2) \underline{\Psi}_0(\ell, \mathbf{t}_1; \lambda) \right] \right] \\ &= \frac{(\lambda - 1) \exp(\ell^2)}{\mathbb{B}(\vartheta)} \left[\frac{\vartheta \mathbf{t}_1^\vartheta}{\Gamma(\vartheta + 1)} + (1 - \vartheta) \right], \\ \eta^2 : \underline{\Psi}_2(\ell, \mathbf{t}_1; \lambda) &= \mathbf{S}^{-1} \left[\frac{1 - \vartheta + \vartheta\left(\frac{\nu}{\xi}\right)^\vartheta}{\mathbb{B}(\vartheta)} \mathbf{S} \left[(\underline{\Psi}_1(\ell, \mathbf{t}_1; \lambda))_{\ell\ell} - (1 + 4\ell^2) \underline{\Psi}_1(\ell, \mathbf{t}_1; \lambda) \right] \right] \\ &= \frac{(\lambda - 1) \exp(\ell^2)}{\mathbb{B}^2(\vartheta)} \left[\frac{\vartheta^2 \mathbf{t}_1^{2\vartheta}}{\Gamma(2\vartheta + 1)} + 2\vartheta(1 - \vartheta) \frac{\mathbf{t}_1^\vartheta}{\Gamma(\vartheta + 1)} + (1 - \vartheta)^2 \right], \\ \eta^3 : \underline{\Psi}_3(\ell, \mathbf{t}_1; \lambda) &= \mathbf{S}^{-1} \left[\frac{1 - \vartheta + \vartheta\left(\frac{\nu}{\xi}\right)^\vartheta}{\mathbb{B}(\vartheta)} \mathbf{S} \left[(\underline{\Psi}_2(\ell, \mathbf{t}_1; \lambda))_{\ell\ell} - (1 + 4\ell^2) \underline{\Psi}_2(\ell, \mathbf{t}_1; \lambda) \right] \right] \\ &= \frac{(\lambda - 1) \exp(\ell^2)}{\mathbb{B}^3(\vartheta)} \left[\frac{\vartheta^3 \mathbf{t}_1^{3\vartheta}}{\Gamma(3\vartheta + 1)} + 3\vartheta^2(1 - \vartheta) \frac{\mathbf{t}_1^{2\vartheta}}{\Gamma(2\vartheta + 1)} + 3\vartheta(1 - \vartheta)^2 \frac{\mathbf{t}_1^\vartheta}{\Gamma(\vartheta + 1)} + (1 - \vartheta)^3 \right], \\ &\vdots \end{aligned}$$

The series form solution is presented as follows:

$$\tilde{\Psi}(\ell, \mathbf{t}_1; \lambda) = \tilde{\Psi}_0(\ell, \mathbf{t}_1; \lambda) + \tilde{\Psi}_1(\ell, \mathbf{t}_1; \lambda) + \tilde{\Psi}_2(\ell, \mathbf{t}_1; \lambda) + \tilde{\Psi}_3(\ell, \mathbf{t}_1; \lambda) + \dots,$$

which implies that:

$$\begin{aligned} \underline{\Psi}(\ell, \mathbf{t}_1; \lambda) &= \underline{\Psi}_0(\ell, \mathbf{t}_1; \lambda) + \underline{\Psi}_1(\ell, \mathbf{t}_1; \lambda) + \underline{\Psi}_2(\ell, \mathbf{t}_1; \lambda) + \underline{\Psi}_3(\ell, \mathbf{t}_1; \lambda) + \dots, \\ \tilde{\Psi}(\ell, \mathbf{t}_1; \lambda) &= \tilde{\Psi}_0(\ell, \mathbf{t}_1; \lambda) + \tilde{\Psi}_1(\ell, \mathbf{t}_1; \lambda) + \tilde{\Psi}_2(\ell, \mathbf{t}_1; \lambda) + \tilde{\Psi}_3(\ell, \mathbf{t}_1; \lambda) + \dots \end{aligned}$$

Finally, we have:

$$\begin{aligned}
\underline{\Psi}(\ell, \mathbf{t}_1; \lambda) &= (\lambda - 1) \exp(\ell^2) \left\{ \begin{aligned} &1 + \frac{1}{\mathbb{B}(\vartheta)} \left[\frac{\vartheta \mathbf{t}_1^\vartheta}{\Gamma(\vartheta+1)} + (1 - \vartheta) \right] \\ &+ \frac{1}{\mathbb{B}^2(\vartheta)} \left[\frac{\vartheta^2 \mathbf{t}_1^{2\vartheta}}{\Gamma(2\vartheta+1)} + 2\vartheta(1 - \vartheta) \frac{\mathbf{t}_1^\vartheta}{\Gamma(\vartheta+1)} + (1 - \vartheta)^2 \right] \\ &+ \frac{1}{\mathbb{B}^3(\vartheta)} \left[\frac{\vartheta^3 \mathbf{t}_1^{3\vartheta}}{\Gamma(3\vartheta+1)} + 3\vartheta^2(1 - \vartheta) \frac{\mathbf{t}_1^{2\vartheta}}{\Gamma(2\vartheta+1)} + 3\vartheta(1 - \vartheta)^2 \frac{\mathbf{t}_1^\vartheta}{\Gamma(\vartheta+1)} + (1 - \vartheta)^3 \right] + \dots, \end{aligned} \right. \\
\bar{\Psi}(\ell, \mathbf{t}_1; \lambda) &= (1 - \lambda) \exp(\ell^2) \left\{ \begin{aligned} &1 + \frac{1}{\mathbb{B}(\vartheta)} \left[\frac{\vartheta \mathbf{t}_1^\vartheta}{\Gamma(\vartheta+1)} + (1 - \vartheta) \right] \\ &+ \frac{1}{\mathbb{B}^2(\vartheta)} \left[\frac{\vartheta^2 \mathbf{t}_1^{2\vartheta}}{\Gamma(2\vartheta+1)} + 2\vartheta(1 - \vartheta) \frac{\mathbf{t}_1^\vartheta}{\Gamma(\vartheta+1)} + (1 - \vartheta)^2 \right] \\ &+ \frac{1}{\mathbb{B}^3(\vartheta)} \left[\frac{\vartheta^3 \mathbf{t}_1^{3\vartheta}}{\Gamma(3\vartheta+1)} + 3\vartheta^2(1 - \vartheta) \frac{\mathbf{t}_1^{2\vartheta}}{\Gamma(2\vartheta+1)} + 3\vartheta(1 - \vartheta)^2 \frac{\mathbf{t}_1^\vartheta}{\Gamma(\vartheta+1)} + (1 - \vartheta)^3 \right] + \dots. \end{aligned} \right.
\end{aligned} \tag{40}$$

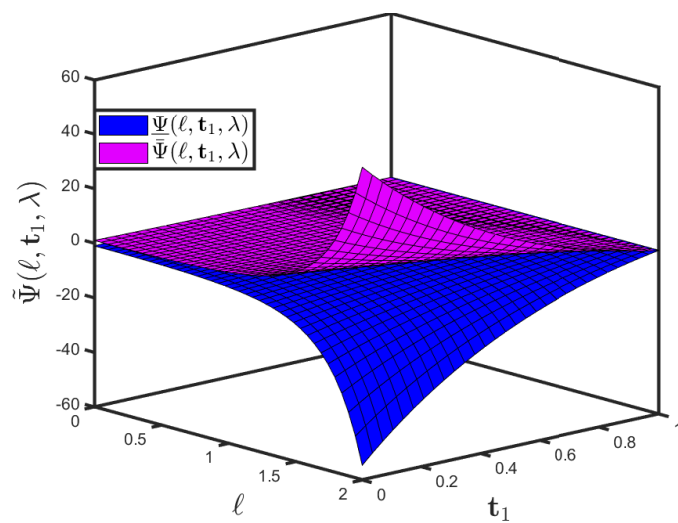
Figure 5a,b reveal how the effectiveness of multiple (lower and upper bound accuracy) surface graphs for Problem 2 interacting with the fuzzy CFD and Shehu transform is being exhibited in this investigation. The pattern specifies the fluctuation in the mapping $\bar{\Psi}(\ell, \mathbf{t}_1; \lambda)$ on the space co-ordinate ℓ with the consideration of \mathbf{t}_1 and the uncertainty parameter $\lambda \in [0, 1]$. The figure illustrates that, as time passes, the mapping $\bar{\Psi}(\ell, \mathbf{t}_1; \lambda)$ will become more intricate.

Figure 6a highlights the impact of the suggested technique on the mapping $\bar{\Psi}(\ell, \mathbf{t}_1; \lambda)$ for the fuzzy CFD to have an uncertainty parameter $\lambda \in [0, 1]$. With the slight increase in $\bar{\Psi}(\ell, \mathbf{t}_1; \lambda)$, it then clearly demonstrates a large decrease in the mapping $\underline{\Psi}(\ell, \mathbf{t}_1; \lambda)$. Figure 6b highlights the effect of the recommended approach on the mapping $\bar{\Psi}(\ell, \mathbf{t}_1; \lambda)$ for the fuzzy CFD to have a fixed fractional order with the varying uncertainty parameter $\lambda \in [0, 1]$. AWith a small increase in the uncertainty parameter, the mappings $\bar{\Psi}(\ell, \mathbf{t}_1; \lambda)$ and $\underline{\Psi}(\ell, \mathbf{t}_1; \lambda)$ are stable.

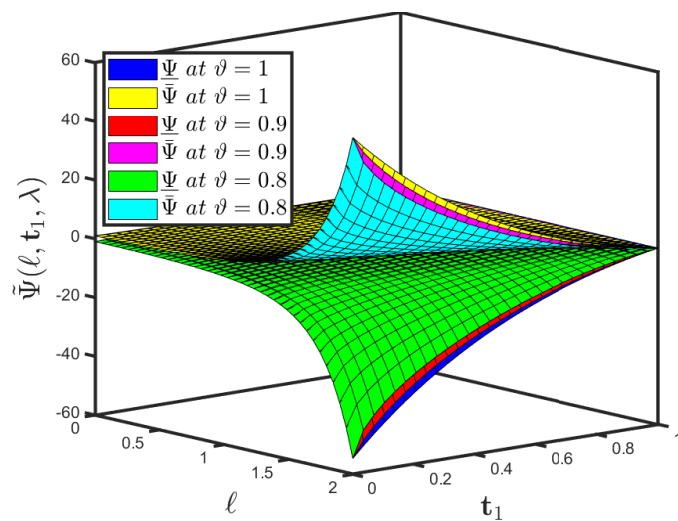
Figure 7a highlights the impact of the suggested technique on the mapping $\bar{\Psi}(\ell, \mathbf{t}_1; \lambda)$ for the fuzzy ABC to have an uncertainty parameter $\lambda \in [0, 1]$. With the slight increase in $\bar{\Psi}(\ell, \mathbf{t}_1; \lambda)$, it then clearly demonstrates a large decrease in the mapping $\underline{\Psi}(\ell, \mathbf{t}_1; \lambda)$. Figure 7b highlights the effect of the recommended approach on the mapping $\bar{\Psi}(\ell, \mathbf{t}_1; \lambda)$ for the fuzzy ABC to have a fixed fractional order with the varying uncertainty parameter $\lambda \in [0, 1]$. With a small increase in the uncertainty parameter, the mappings $\bar{\Psi}(\ell, \mathbf{t}_1; \lambda)$ and $\underline{\Psi}(\ell, \mathbf{t}_1; \lambda)$ are stable.

Figure 8a,b illustrate the comparison between the lower and upper bound accuracies for fuzzy CFD and fuzzy ABC fractional derivative operators for Problem 2 established by the SHPTM for standard motion, i.e., at $\vartheta = 1$.

The graphs in Figures 5–8 assist in recognizing how time and space variation statistically interact. In addition, the proposed method will facilitate scientists' work on pattern formation, diffusion, instability theory, and monitoring competence by employing inferential statistical testing.

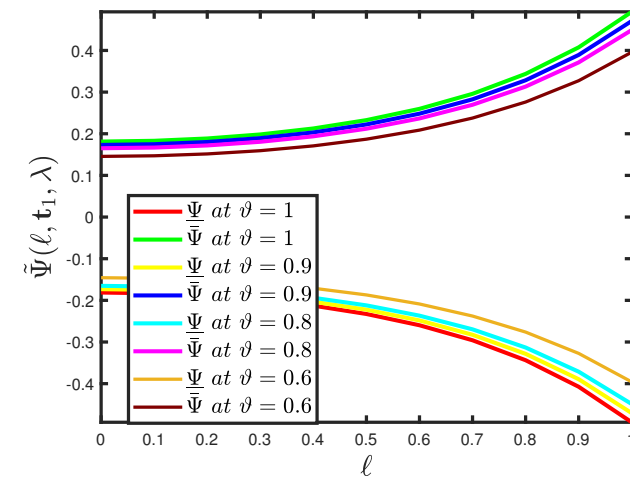


(a)

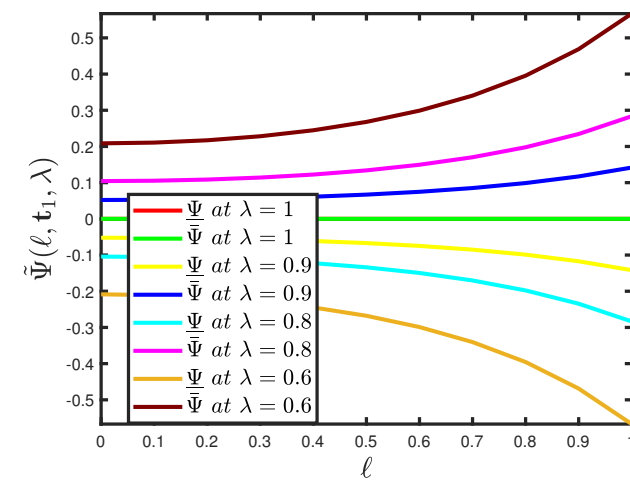


(b)

Figure 5. Three-dimensional plot of $\tilde{\Psi}(\ell, t_1; \lambda)$ of Problem (2): (a) $\Psi(\ell, t_1; \lambda)$ and $\tilde{\Psi}(\ell, t_1; \lambda)$ when $\vartheta = 1$; and (b) $\Psi(\ell, t_1; \lambda)$ and $\tilde{\Psi}(\ell, t_1; \lambda)$ when the uncertainty parameter $\lambda \in [0, 1]$ has different fractional orders.



(a)



(b)

Figure 6. Two-dimensional simulation of $\tilde{\Psi}(\ell, \mathbf{t}_1; \lambda)$ of Problem (2): (a) $\underline{\Psi}(\ell, \mathbf{t}_1; \lambda)$ and $\tilde{\Psi}(\ell, \mathbf{t}_1; \lambda)$ when fuzzy CFD is considered to have an uncertainty parameter $\lambda \in [0, 1]$ and $\mathbf{t}_1 = 0.7$; and (b) $\underline{\Psi}(\ell, \mathbf{t}_1; \lambda)$ and $\tilde{\Psi}(\ell, \mathbf{t}_1; \lambda)$ when fuzzy CFD is considered to have a fractional order $\vartheta = 0.7$ and $\mathbf{t}_1 = 0.7$.

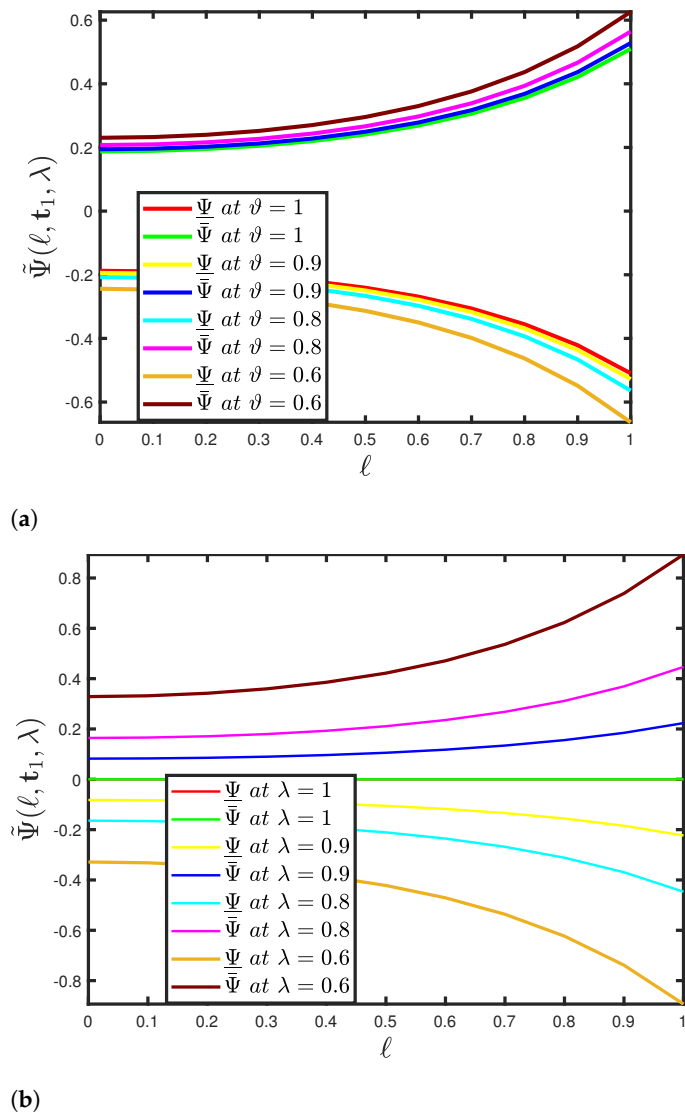
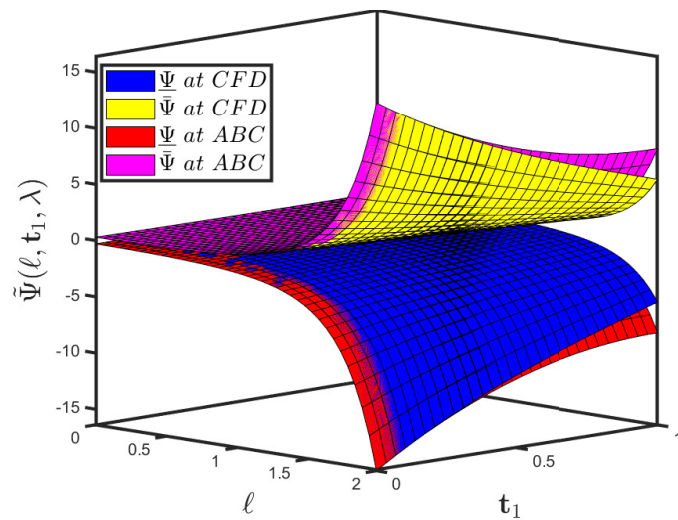
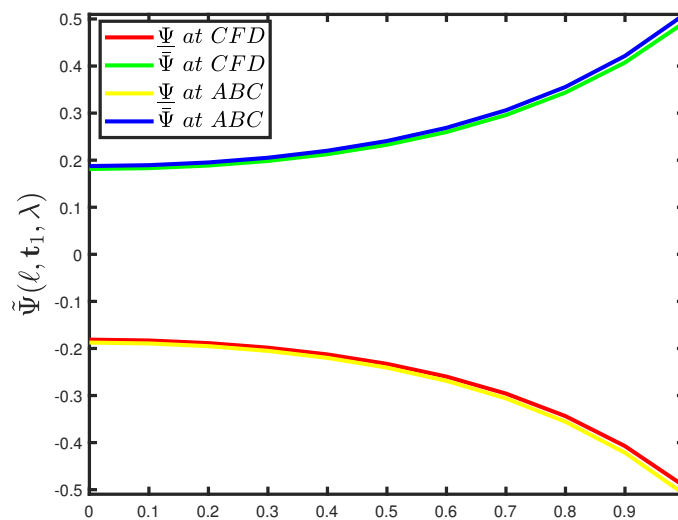


Figure 7. Two-dimensional simulation of $\tilde{\Psi}(\ell, \mathbf{t}_1; \lambda)$ of Problem (2): (a) $\Psi(\ell, \mathbf{t}_1; \lambda)$ and $\tilde{\Psi}(\ell, \mathbf{t}_1; \lambda)$ when fuzzy ABC is considered to have an uncertainty parameter $\lambda \in [0, 1]$ and $\mathbf{t}_1 = 0.7$; and (b) $\Psi(\ell, \mathbf{t}_1; \lambda)$ and $\tilde{\Psi}(\ell, \mathbf{t}_1; \lambda)$ when fuzzy ABC is considered to have a fractional order $\vartheta = 0.7$ and $\mathbf{t}_1 = 0.7$.



(a)



(b)

Figure 8. Comparison plots of $\tilde{\Psi}(\ell, t_1; \lambda)$ of Problem (2) when fuzzy CFD and ABC are considered to have a fractional order $\vartheta = 1$ and uncertainty parameter $\lambda \in [0, 1]$: (a) three-dimensional plot; (b) two-dimensional plot of $\underline{\Psi}(\ell, t_1; \lambda)$ and $\tilde{\Psi}(\ell, t_1; \lambda)$ when $t_1 = 0.7$

Remark 3. When $[\lambda - 1, 1 - \lambda] = 1$ and $\vartheta = 1$, then solution (40) reduces to the integer-order solution $\Psi(\ell, t_1) = \exp(\ell^2 + t_1)$.

Problem 3. Assume the fuzzy time-fractional Cauchy-reaction diffusion model:

$$\frac{\partial^\vartheta}{\partial t_1^\vartheta} \tilde{\Psi}(\ell, t_1; \lambda) = \frac{\partial^2}{\partial \ell^2} \tilde{\Psi}(\ell, t_1; \lambda) \oplus 2 \odot t_1 \odot \tilde{\Psi}(\ell, t_1; \lambda), \quad 0 < \vartheta \leq 1, \quad (41)$$

subject to the fuzzy initial condition:

$$\tilde{\Psi}(\ell, 0) = \tilde{Y}(\lambda) \odot \exp(\ell), \quad (42)$$

where $\tilde{Y}(\lambda) = [\underline{Y}(\lambda), \bar{Y}(\lambda)] = [\lambda - 1, 1 - \lambda]$ for $\lambda \in [0, 1]$ is the fuzzy number.

The parameterized formulation of (44) is presented as

$$\begin{cases} \frac{\partial^\vartheta}{\partial \mathbf{t}_1^\vartheta} \underline{\Psi}(\ell, \mathbf{t}_1; \lambda) = \frac{\partial^2}{\partial \ell^2} \underline{\Psi}(\ell, \mathbf{t}_1; \lambda) + 2\mathbf{t}_1 \underline{\Psi}(\ell, \mathbf{t}_1; \lambda), \\ \underline{\Psi}(\ell, 0) = (\lambda - 1) \exp(\ell) \\ \frac{\partial^\vartheta}{\partial \mathbf{t}_1^\vartheta} \underline{\Psi}(\ell, \mathbf{t}_1; \lambda) = \frac{\partial^2}{\partial \ell^2} \underline{\Psi}(\ell, \mathbf{t}_1; \lambda) + 2\mathbf{t}_1 \underline{\Psi}(\ell, \mathbf{t}_1; \lambda), \\ \underline{\Psi}(\ell, 0) = (1 - \lambda) \exp(\ell). \end{cases}$$

Case 1. Firstly, we take into consideration the CFD coupled with the Shehu homotopy perturbation transform method in the first case of (46). Considering the process stated in Section, we have:

$$\left(\frac{\nu}{\xi}\right)^\vartheta \mathbf{S}[\underline{\Psi}(\ell, \mathbf{t}_1; \lambda)] - \sum_{\kappa=0}^{r-1} \left(\frac{\xi}{\nu}\right)^{\vartheta-\kappa-1} \underline{\Psi}^{(\kappa)}(0) = \mathbf{S} \left[\frac{\partial^2}{\partial \ell^2} \underline{\Psi}(\ell, \mathbf{t}_1; \lambda) + 2\mathbf{t}_1 \underline{\Psi}(\ell, \mathbf{t}_1; \lambda) \right].$$

Considering the fuzzy initial condition, making use of the inverse Shehu transform implies that:

$$\underline{\Psi}(\ell, \mathbf{t}_1; \lambda) = \frac{\nu}{\xi} (\lambda - 1) \exp(\ell) + \mathbf{S}^{-1} \left[\left(\frac{\nu}{\xi}\right)^\vartheta \mathbf{S} \left[\frac{\partial^2}{\partial \ell^2} \underline{\Psi}(\ell, \mathbf{t}_1; \lambda) + 2\mathbf{t}_1 \underline{\Psi}(\ell, \mathbf{t}_1; \lambda) \right] \right].$$

Now, by implementing the HPM, we have:

$$\sum_{\kappa=0}^{+\infty} \eta^\kappa \underline{\Psi}_\kappa(\ell, \mathbf{t}_1; \lambda) = (\lambda - 1) \exp(\ell) + \eta \left(\mathbf{S}^{-1} \left[\left(\frac{\nu}{\xi}\right)^\vartheta \mathbf{S} \left[\left(\sum_{\kappa=0}^{+\infty} \eta^\kappa \underline{\Psi}_\kappa(\ell, \mathbf{t}_1; \lambda) \right)_{\ell\ell} + 2\mathbf{t}_1 \left(\sum_{\kappa=0}^{+\infty} \eta^\kappa \underline{\Psi}_\kappa(\ell, \mathbf{t}_1; \lambda) \right) \right] \right] \right).$$

Equating the coefficients of the same powers of η , we have:

$$\begin{aligned} \eta^0 : \underline{\Psi}_0(\ell, \mathbf{t}_1; \lambda) &= (\lambda - 1) \exp(\ell), \\ \eta^1 : \underline{\Psi}_1(\ell, \mathbf{t}_1; \lambda) &= \mathbf{S}^{-1} \left[\left(\frac{\nu}{\xi}\right)^\vartheta \mathbf{S} \left[(\underline{\Psi}_0(\ell, \mathbf{t}_1; \lambda))_{\ell\ell} + 2\mathbf{t}_1 \underline{\Psi}_0(\ell, \mathbf{t}_1; \lambda) \right] \right] = (\lambda - 1) \exp(\ell) \left[\frac{\mathbf{t}_1^\vartheta}{\Gamma(\vartheta + 1)} + \frac{2\mathbf{t}_1^{\vartheta+1}}{\Gamma(\vartheta + 2)} \right], \\ \eta^2 : \underline{\Psi}_1(\ell, \mathbf{t}_1; \lambda) &= \mathbf{S}^{-1} \left[\left(\frac{\nu}{\xi}\right)^\vartheta \mathbf{S} \left[(\underline{\Psi}_1(\ell, \mathbf{t}_1; \lambda))_{\ell\ell} + 2\mathbf{t}_1 \underline{\Psi}_1(\ell, \mathbf{t}_1; \lambda) \right] \right] \\ &= (\lambda - 1) \exp(\ell) \left[\frac{\mathbf{t}_1^{2\vartheta}}{\Gamma(2\vartheta + 1)} + 2(\vartheta + 2) \frac{\mathbf{t}_1^{2\vartheta+1}}{\Gamma(2\vartheta + 2)} + 4(\vartheta + 2) \frac{\mathbf{t}_1^{2\vartheta+2}}{\Gamma(2\vartheta + 3)} \right], \\ \eta^3 : \underline{\Psi}_2(\ell, \mathbf{t}_1; \lambda) &= \mathbf{S}^{-1} \left[\left(\frac{\nu}{\xi}\right)^\vartheta \mathbf{S} \left[(\underline{\Psi}_2(\ell, \mathbf{t}_1; \lambda))_{\ell\ell} + 2\mathbf{t}_1 \underline{\Psi}_2(\ell, \mathbf{t}_1; \lambda) \right] \right] \\ &= (\lambda - 1) \exp(\ell) \left[\frac{\mathbf{t}_1^{3\vartheta}}{\Gamma(3\vartheta + 1)} + 6(\vartheta + 1) \frac{\mathbf{t}_1^{3\vartheta+1}}{\Gamma(3\vartheta + 2)} + 4(\vartheta + 2)(\vartheta + 3) \frac{\mathbf{t}_1^{3\vartheta+2}}{\Gamma(3\vartheta + 3)} \right. \\ &\quad \left. + 8(\vartheta + 2)(2\vartheta + 3) \frac{\mathbf{t}_1^{3\vartheta+3}}{\Gamma(3\vartheta + 4)} \right], \\ &\vdots \end{aligned}$$

The series form solution is presented as follows:

$$\underline{\Psi}(\ell, \mathbf{t}_1; \lambda) = \underline{\Psi}_0(\ell, \mathbf{t}_1; \lambda) + \underline{\Psi}_1(\ell, \mathbf{t}_1; \lambda) + \underline{\Psi}_2(\ell, \mathbf{t}_1; \lambda) + \underline{\Psi}_3(\ell, \mathbf{t}_1; \lambda) + \dots,$$

which implies that:

$$\begin{aligned} \underline{\Psi}(\ell, \mathbf{t}_1; \lambda) &= \underline{\Psi}_0(\ell, \mathbf{t}_1; \lambda) + \underline{\Psi}_1(\ell, \mathbf{t}_1; \lambda) + \underline{\Psi}_2(\ell, \mathbf{t}_1; \lambda) + \underline{\Psi}_3(\ell, \mathbf{t}_1; \lambda) + \dots, \\ \underline{\Psi}(\ell, \mathbf{t}_1; \lambda) &= \underline{\Psi}_0(\ell, \mathbf{t}_1; \lambda) + \underline{\Psi}_1(\ell, \mathbf{t}_1; \lambda) + \underline{\Psi}_2(\ell, \mathbf{t}_1; \lambda) + \underline{\Psi}_3(\ell, \mathbf{t}_1; \lambda) + \dots. \end{aligned}$$

Finally, we have:

$$\begin{aligned} \underline{\Psi}(\ell, \mathbf{t}_1; \lambda) &= (\lambda - 1) \exp(\ell) \left\{ \begin{aligned} &1 + \left[\frac{\mathbf{t}_1^\vartheta}{\Gamma(\vartheta+1)} + 2 \frac{\mathbf{t}_1^{\vartheta+1}}{\Gamma(\vartheta+2)} \right] \\ &+ \left[\frac{\mathbf{t}_1^{2\vartheta}}{\Gamma(2\vartheta+1)} + 2(\vartheta + 2) \frac{\mathbf{t}_1^{2\vartheta+1}}{\Gamma(2\vartheta+2)} + 4(\vartheta + 2) \frac{\mathbf{t}_1^{2\vartheta+2}}{\Gamma(2\vartheta+3)} \right] \\ &+ \left[\frac{\mathbf{t}_1^{3\vartheta}}{\Gamma(3\vartheta+1)} + 6(\vartheta + 1) \frac{\mathbf{t}_1^{3\vartheta+1}}{\Gamma(3\vartheta+2)} + 4(\vartheta + 2)(\vartheta + 3) \frac{\mathbf{t}_1^{3\vartheta+2}}{\Gamma(3\vartheta+3)} \right. \\ &\left. + 8(\vartheta + 2)(2\vartheta + 3) \frac{\mathbf{t}_1^{3\vartheta+3}}{\Gamma(3\vartheta+4)} \right] + \dots, \end{aligned} \right. \\ \underline{\Psi}(\ell, \mathbf{t}_1; \lambda) &= (1 - \lambda) \exp(\ell) \left\{ \begin{aligned} &1 + \left[\frac{\mathbf{t}_1^\vartheta}{\Gamma(\vartheta+1)} + 2 \frac{\mathbf{t}_1^{\vartheta+1}}{\Gamma(\vartheta+2)} \right] \\ &+ \left[\frac{\mathbf{t}_1^{2\vartheta}}{\Gamma(2\vartheta+1)} + 2(\vartheta + 2) \frac{\mathbf{t}_1^{2\vartheta+1}}{\Gamma(2\vartheta+2)} + 4(\vartheta + 2) \frac{\mathbf{t}_1^{2\vartheta+2}}{\Gamma(2\vartheta+3)} \right] \\ &+ \left[\frac{\mathbf{t}_1^{3\vartheta}}{\Gamma(3\vartheta+1)} + 6(\vartheta + 1) \frac{\mathbf{t}_1^{3\vartheta+1}}{\Gamma(3\vartheta+2)} + 4(\vartheta + 2)(\vartheta + 3) \frac{\mathbf{t}_1^{3\vartheta+2}}{\Gamma(3\vartheta+3)} \right. \\ &\left. + 8(\vartheta + 2)(2\vartheta + 3) \frac{\mathbf{t}_1^{3\vartheta+3}}{\Gamma(3\vartheta+4)} \right] + \dots. \end{aligned} \right. \end{aligned}$$

Case 2. Now, we employ the ABC derivative operator in the first case of (37) as follows.

Considering the process stated in Section 3, we have:

$$\frac{\mathbb{B}(\vartheta)}{1 - \vartheta + \vartheta(\frac{\nu}{\xi})^\vartheta} \mathbf{S}[\underline{\Psi}(\ell, \mathbf{t}_1; \lambda)] - \frac{\mathbb{B}(\vartheta)}{1 - \vartheta + \vartheta(\frac{\nu}{\xi})^\vartheta} \left(\frac{\nu}{\xi}\right) \underline{\Psi}(\ell, 0) = \mathbf{S} \left[\frac{\partial^2}{\partial \ell^2} \underline{\Psi}(\ell, \mathbf{t}_1; \lambda) + 2\mathbf{t}_1 \underline{\Psi}(\ell, \mathbf{t}_1; \lambda) \right].$$

Considering the fuzzy initial condition, making use of the inverse Shehu transform implies that:

$$\underline{\Psi}(\ell, \mathbf{t}_1; \lambda) = \frac{\nu}{\xi} (\lambda - 1) \exp(\ell) + \mathbf{S}^{-1} \left[\frac{1 - \vartheta + \vartheta(\frac{\nu}{\xi})^\vartheta}{\mathbb{B}(\vartheta)} \mathbf{S} \left[\frac{\partial^2}{\partial \ell^2} \underline{\Psi}(\ell, \mathbf{t}_1; \lambda) + 2\mathbf{t}_1 \underline{\Psi}(\ell, \mathbf{t}_1; \lambda) \right] \right].$$

Now, by implementing the HPM, we have:

$$\sum_{\kappa=0}^{+\infty} \eta^\kappa \underline{\Psi}_\kappa(\ell, \mathbf{t}_1; \lambda) = (\lambda - 1) \exp(\ell) + \eta \left(\mathbf{S}^{-1} \left[\frac{1 - \vartheta + \vartheta(\frac{\nu}{\xi})^\vartheta}{\mathbb{B}(\vartheta)} \mathbf{S} \left[\left(\sum_{\kappa=0}^{+\infty} \eta^\kappa \underline{\Psi}_\kappa(\ell, \mathbf{t}_1; \lambda) \right)_{\ell\ell} + 2\mathbf{t}_1 \left(\sum_{\kappa=0}^{+\infty} \eta^\kappa \underline{\Psi}_\kappa(\ell, \mathbf{t}_1; \lambda) \right) \right] \right] \right).$$

Equating the coefficients of the same powers of η , we have:

$$\begin{aligned} \eta^0 : \underline{\Psi}_0(\ell, \mathbf{t}_1; \lambda) &= (\lambda - 1) \exp(\ell), \\ \eta^1 : \underline{\Psi}_1(\ell, \mathbf{t}_1; \lambda) &= \mathbf{S}^{-1} \left[\frac{1 - \vartheta + \vartheta(\frac{\nu}{\xi})^\vartheta}{\mathbb{B}(\vartheta)} \mathbf{S} \left[(\underline{\Psi}_0(\ell, \mathbf{t}_1; \lambda))_{\ell\ell} + 2\mathbf{t}_1 \underline{\Psi}_0(\ell, \mathbf{t}_1; \lambda) \right] \right] \\ &= \frac{(\lambda - 1) \exp(\ell)}{\mathbb{B}(\vartheta)} \left[\frac{2\vartheta \mathbf{t}_1^{\vartheta+1}}{\Gamma(\vartheta + 2)} + \frac{\vartheta \mathbf{t}_1^\vartheta}{\Gamma(\vartheta + 1)} + 2\mathbf{t}_1(1 - \vartheta) + (1 - \vartheta) \right], \\ \eta^2 : \underline{\Psi}_2(\ell, \mathbf{t}_1; \lambda) &= \mathbf{S}^{-1} \left[\frac{1 - \vartheta + \vartheta(\frac{\nu}{\xi})^\vartheta}{\mathbb{B}(\vartheta)} \mathbf{S} \left[(\underline{\Psi}_1(\ell, \mathbf{t}_1; \lambda))_{\ell\ell} + 2\mathbf{t}_1 \underline{\Psi}_1(\ell, \mathbf{t}_1; \lambda) \right] \right] \\ &= \frac{(\lambda - 1) \exp(\ell)}{\mathbb{B}^2(\vartheta)} \left[4\vartheta(\vartheta + 2) \frac{\mathbf{t}_1^{2\vartheta+2}}{\Gamma(2\vartheta + 3)} + 2\vartheta(\vartheta + 2) \frac{\mathbf{t}_1^{2\vartheta+1}}{\Gamma(2\vartheta + 1)} + \vartheta \frac{\mathbf{t}_1^{2\vartheta}}{\Gamma(2\vartheta + 1)} + 8(1 - \vartheta) \frac{\mathbf{t}_1^{\vartheta+2}}{\Gamma(\vartheta + 3)} \right. \\ &\quad \left. + 4(1 - \vartheta) \frac{\mathbf{t}_1^{\vartheta+1}}{\Gamma(\vartheta + 2)} + (1 - \vartheta) \frac{\mathbf{t}_1^\vartheta}{\Gamma(\vartheta + 1)} \right], \\ &\vdots \end{aligned}$$

The series form solution is presented as follows:

$$\tilde{\Psi}(\ell, \mathbf{t}_1; \lambda) = \tilde{\Psi}_0(\ell, \mathbf{t}_1; \lambda) + \tilde{\Psi}_1(\ell, \mathbf{t}_1; \lambda) + \tilde{\Psi}_2(\ell, \mathbf{t}_1; \lambda) + \tilde{\Psi}_3(\ell, \mathbf{t}_1; \lambda) + \dots,$$

which implies that:

$$\begin{aligned}\underline{\Psi}(\ell, \mathbf{t}_1; \lambda) &= \underline{\Psi}_0(\ell, \mathbf{t}_1; \lambda) + \underline{\Psi}_1(\ell, \mathbf{t}_1; \lambda) + \underline{\Psi}_2(\ell, \mathbf{t}_1; \lambda) + \underline{\Psi}_3(\ell, \mathbf{t}_1; \lambda) + \dots, \\ \bar{\Psi}(\ell, \mathbf{t}_1; \lambda) &= \bar{\Psi}_0(\ell, \mathbf{t}_1; \lambda) + \bar{\Psi}_1(\ell, \mathbf{t}_1; \lambda) + \bar{\Psi}_2(\ell, \mathbf{t}_1; \lambda) + \bar{\Psi}_3(\ell, \mathbf{t}_1; \lambda) + \dots.\end{aligned}$$

Finally, we have:

$$\begin{aligned}\underline{\Psi}(\ell, \mathbf{t}_1; \lambda) &= (\lambda - 1) \exp(\ell) \left\{ \begin{aligned} &1 + \frac{1}{\mathbb{B}(\vartheta)} \left[\frac{2\vartheta \mathbf{t}_1^{\vartheta+1}}{\Gamma(\vartheta+2)} + \frac{\vartheta \mathbf{t}_1^{\vartheta}}{\Gamma(\vartheta+1)} + 2\mathbf{t}_1(1 - \vartheta) + (1 - \vartheta) \right] \\ &+ \frac{1}{\mathbb{B}^2(\vartheta)} \left[4\vartheta(\vartheta + 2) \frac{\mathbf{t}_1^{2\vartheta+2}}{\Gamma(2\vartheta+3)} + 2\vartheta(\vartheta + 2) \frac{\mathbf{t}_1^{2\vartheta+1}}{\Gamma(2\vartheta+2)} + \vartheta \frac{\mathbf{t}_1^{2\vartheta}}{\Gamma(2\vartheta+1)} + 8(1 - \vartheta) \frac{\mathbf{t}_1^{\vartheta+2}}{\Gamma(\vartheta+3)} \right. \\ &\left. + 4(1 - \vartheta) \frac{\mathbf{t}_1^{\vartheta+1}}{\Gamma(\vartheta+2)} + (1 - \vartheta) \frac{\mathbf{t}_1^{\vartheta}}{\Gamma(\vartheta+1)} \right] + \dots, \end{aligned} \right. \\ \bar{\Psi}(\ell, \mathbf{t}_1; \lambda) &= (1 - \lambda) \exp(\ell) \left\{ \begin{aligned} &1 + \frac{1}{\mathbb{B}(\vartheta)} \left[\frac{2\vartheta \mathbf{t}_1^{\vartheta+1}}{\Gamma(\vartheta+2)} + \frac{\vartheta \mathbf{t}_1^{\vartheta}}{\Gamma(\vartheta+1)} + 2\mathbf{t}_1(1 - \vartheta) + (1 - \vartheta) \right] \\ &+ \frac{1}{\mathbb{B}^2(\vartheta)} \left[4\vartheta(\vartheta + 2) \frac{\mathbf{t}_1^{2\vartheta+2}}{\Gamma(2\vartheta+3)} + 2\vartheta(\vartheta + 2) \frac{\mathbf{t}_1^{2\vartheta+1}}{\Gamma(2\vartheta+2)} + \vartheta \frac{\mathbf{t}_1^{2\vartheta}}{\Gamma(2\vartheta+1)} + 8(1 - \vartheta) \frac{\mathbf{t}_1^{\vartheta+2}}{\Gamma(\vartheta+3)} \right. \\ &\left. + 4(1 - \vartheta) \frac{\mathbf{t}_1^{\vartheta+1}}{\Gamma(\vartheta+2)} + (1 - \vartheta) \frac{\mathbf{t}_1^{\vartheta}}{\Gamma(\vartheta+1)} \right] + \dots. \end{aligned} \right. \end{aligned} \quad (43)$$

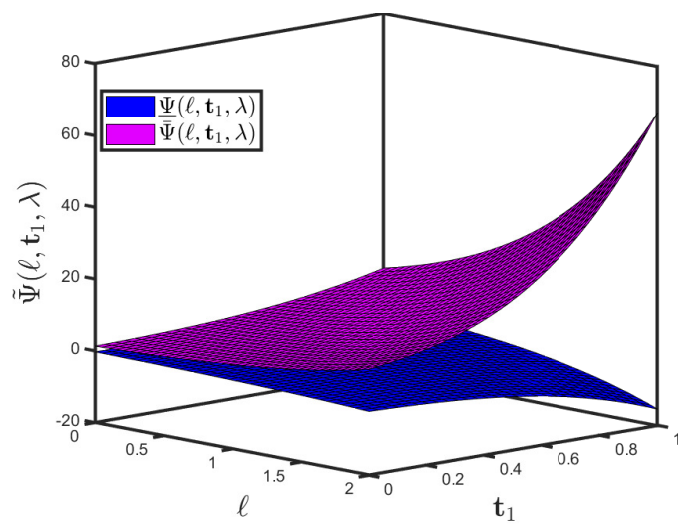
Figure 9a,b reveal how the effectiveness of multiple (lower and upper bound accuracy) surface graphs for Problem 2 interacting with the fuzzy CFD and Shehu transform is being exhibited in this investigation. The pattern specifies the fluctuation in the mapping $\bar{\Psi}(\ell, \mathbf{t}_1; \lambda)$ on the space co-ordinate ℓ with the consideration of \mathbf{t}_1 and the uncertainty parameter $\lambda \in [0, 1]$. The figure illustrates that, as time passes, the mapping $\bar{\Psi}(\ell, \mathbf{t}_1; \lambda)$ will become more intricate.

Figure 10a highlights the impact of the suggested technique on the mapping $\bar{\Psi}(\ell, \mathbf{t}_1; \lambda)$ for the fuzzy CFD to have an uncertainty parameter $\lambda \in [0, 1]$. With the slight increase in $\bar{\Psi}(\ell, \mathbf{t}_1; \lambda)$, it then clearly demonstrates a large decrease in the mapping $\underline{\Psi}(\ell, \mathbf{t}_1; \lambda)$. Figure 10b highlights the effect of the recommended approach on the mapping $\bar{\Psi}(\ell, \mathbf{t}_1; \lambda)$ for the fuzzy CFD to have a fixed fractional order with the varying uncertainty parameter $\lambda \in [0, 1]$. With a small increase in the uncertainty parameter, the mappings $\bar{\Psi}(\ell, \mathbf{t}_1; \lambda)$ and $\underline{\Psi}(\ell, \mathbf{t}_1; \lambda)$ are stable.

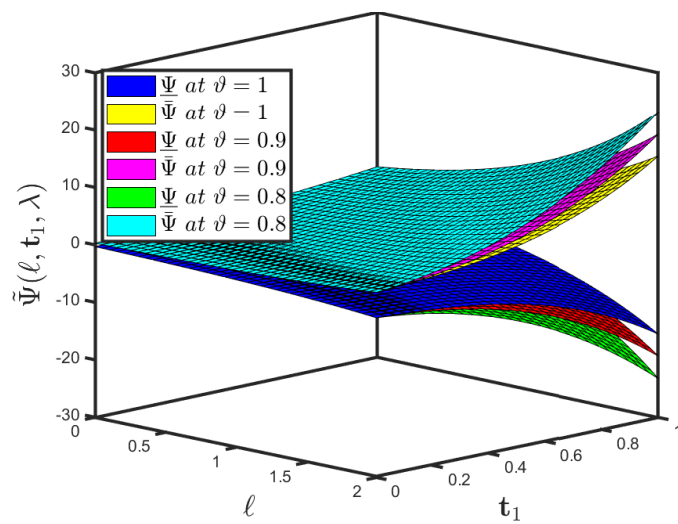
Figure 11a highlights the impact of the suggested technique on the mapping $\bar{\Psi}(\ell, \mathbf{t}_1; \lambda)$ for the fuzzy ABC to have an uncertainty parameter $\lambda \in [0, 1]$. With the slight increase in $\bar{\Psi}(\ell, \mathbf{t}_1; \lambda)$, it then clearly demonstrates a large decrease in the mapping $\underline{\Psi}(\ell, \mathbf{t}_1; \lambda)$. Figure 11b highlights the effect of the recommended approach on the mapping $\bar{\Psi}(\ell, \mathbf{t}_1; \lambda)$ for the fuzzy ABC to have a fixed fractional order with the varying uncertainty parameter $\lambda \in [0, 1]$. With a small increase in the uncertainty parameter, the mappings $\bar{\Psi}(\ell, \mathbf{t}_1; \lambda)$ and $\underline{\Psi}(\ell, \mathbf{t}_1; \lambda)$ are stable.

Figure 12a,b illustrate the comparison between the lower and upper bound accuracies for fuzzy CFD and fuzzy ABC fractional derivative operators for Problem 3 established by the SHPTM for standard motion, i.e., at $\vartheta = 1$.

The graphs in Figures 9–12 assist in recognizing how time and space variation statistically interact. In addition, the proposed method will facilitate scientists' work on pattern formation, diffusion, instability theory, and monitoring competence by employing inferential statistical testing.

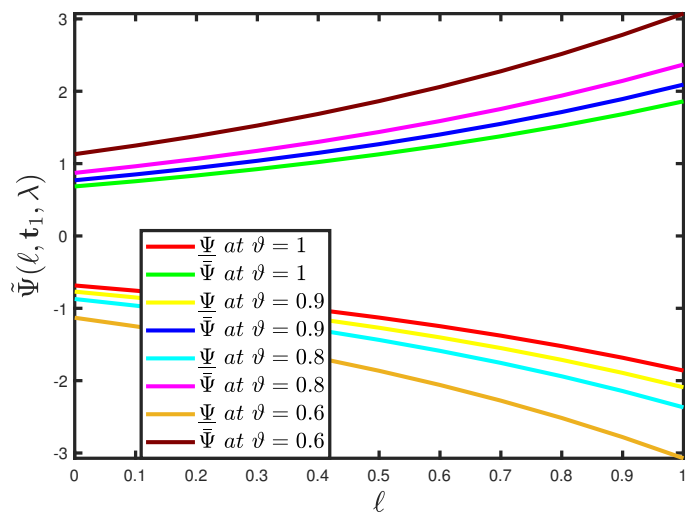


(a)

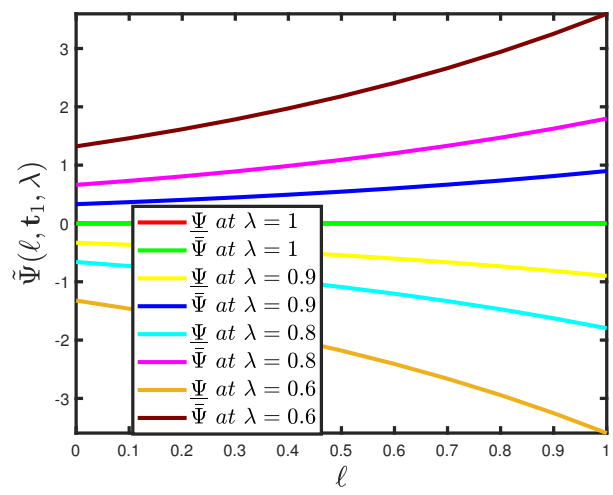


(b)

Figure 9. (a) Three-dimensional plot of $\tilde{\Psi}(\ell, t_1; \lambda)$ of Problem (3): (a) $\underline{\Psi}(\ell, t_1; \lambda)$ and $\bar{\Psi}(\ell, t_1; \lambda)$ when $\vartheta = 1$; and (b) $\underline{\Psi}(\ell, t_1; \lambda)$ and $\bar{\Psi}(\ell, t_1; \lambda)$ when the uncertainty parameter $\lambda \in [0, 1]$ has different fractional orders.

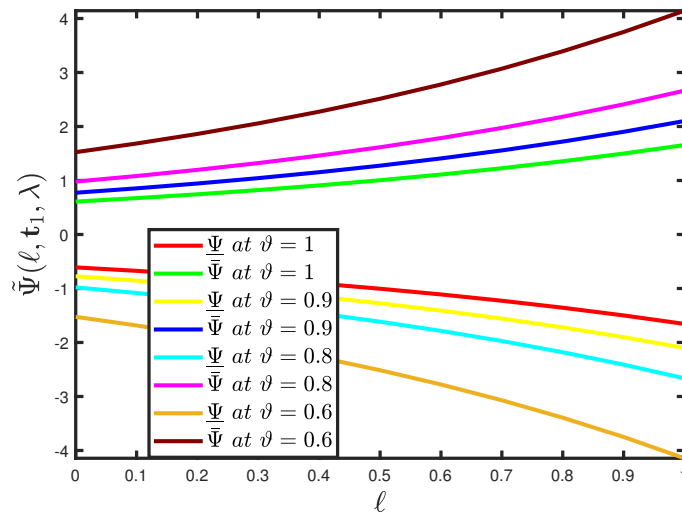


(a)

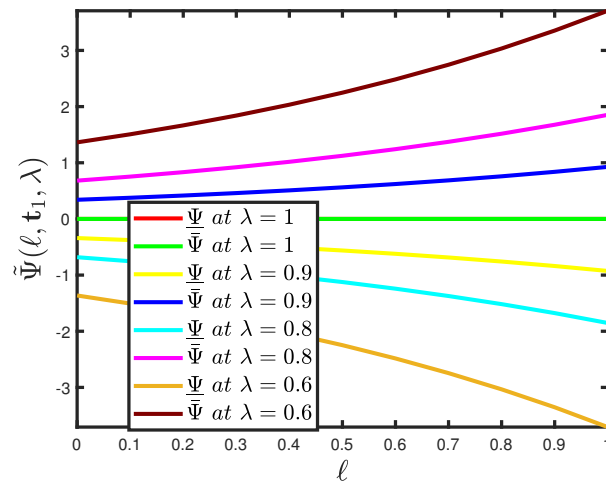


(b)

Figure 10. Two-dimensional simulation of $\tilde{\Psi}(\ell, t_1; \lambda)$ of Problem (3): (a) $\underline{\Psi}(\ell, t_1; \lambda)$ and $\tilde{\Psi}(\ell, t_1; \lambda)$ when fuzzy CFD is considered to have an uncertainty parameter $\lambda \in [0, 1]$ and $t_1 = 0.7$; and (b) $\underline{\Psi}(\ell, t_1; \lambda)$ and $\tilde{\Psi}(\ell, t_1; \lambda)$ when fuzzy CFD is considered to have a fractional order $\vartheta = 0.7$ and $t_1 = 0.7$.

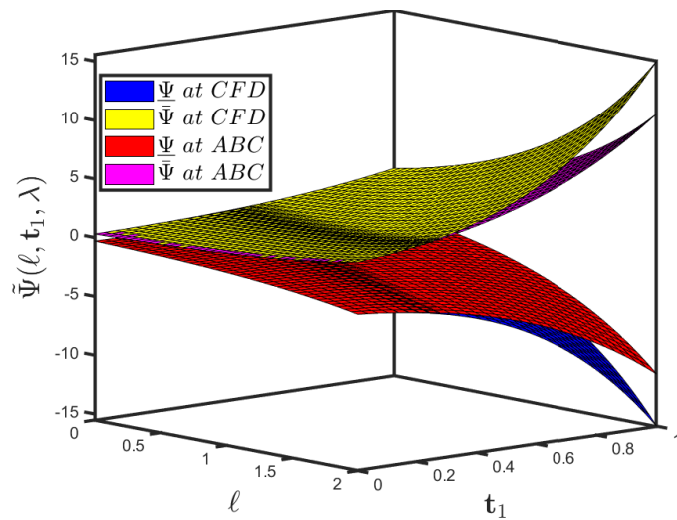


(a)

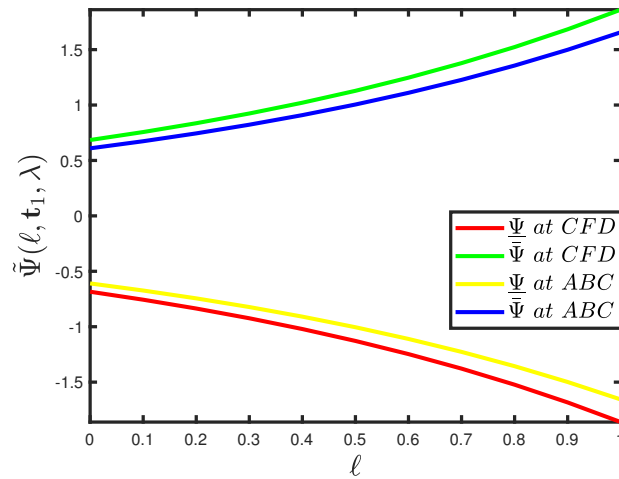


(b)

Figure 11. Two-dimensional simulation of $\tilde{\Psi}(\ell, t_1; \lambda)$ of Problem (3): (a) $\underline{\Psi}(\ell, t_1; \lambda)$ and $\bar{\Psi}(\ell, t_1; \lambda)$ when fuzzy ABC is considered to have an uncertainty parameter $\lambda \in [0, 1]$ and $t_1 = 0.7$; and (b) $\underline{\Psi}(\ell, t_1; \lambda)$ and $\bar{\Psi}(\ell, t_1; \lambda)$ when fuzzy ABC is considered to have a fractional order $\vartheta = 0.7$ and $t_1 = 0.7$.



(a)



(b)

Figure 12. Comparison plots of $\tilde{\Psi}(\ell, t_1; \lambda)$ of Problem (3) when fuzzy CFD and ABC are considered to have a fractional order $\vartheta = 1$ and uncertainty parameter $\lambda \in [0, 1]$: (a) three-dimensional plot; and (b) two-dimensional plot of $\underline{\Psi}(\ell, t_1; \lambda)$ and $\overline{\Psi}(\ell, t_1; \lambda)$ when $t_1 = 0.7$.

Remark 4. When $[\lambda - 1, 1 - \lambda] = 1$ and $\vartheta = 1$, then solution (43) reduces to the integer-order solution $\Psi(\ell, t_1) = \exp(\ell + t_1 + t_1^2)$.

Problem 4. Assume that the fuzzy time-fractional Cauchy-reaction diffusion model:

$$\frac{\partial^\vartheta}{\partial t_1^\vartheta} \tilde{\Psi}(\ell, t_1; \lambda) = \frac{\partial^2}{\partial \ell^2} \tilde{\Psi}(\ell, t_1; \lambda) \ominus (4 \odot \ell^2 \ominus 2 \odot t_1 \oplus 2) \tilde{\Psi}(\ell, t_1; \lambda), \quad 0 < \vartheta \leq 1, \quad (44)$$

is subject to the fuzzy initial condition:

$$\tilde{\Psi}(\ell, 0) = \tilde{Y}(\lambda) \odot \exp(\ell^2), \quad (45)$$

where $\tilde{Y}(\lambda) = [\underline{Y}(\lambda), \overline{Y}(\lambda)] = [\lambda - 1, 1 - \lambda]$ for $\lambda \in [0, 1]$ is a fuzzy number.

The parameterized formulation of (44) is presented as

$$\begin{cases} \frac{\partial^\vartheta}{\partial \mathbf{t}_1^\vartheta} \underline{\Psi}(\ell, \mathbf{t}_1; \lambda) = \frac{\partial^2}{\partial \ell^2} \underline{\Psi}(\ell, \mathbf{t}_1; \lambda) - (4\ell^2 - 2\mathbf{t}_1 + 2)\underline{\Psi}(\ell, \mathbf{t}_1; \lambda), \\ \underline{\Psi}(\ell, 0) = (\lambda - 1) \exp(\ell^2) \\ \frac{\partial^\vartheta}{\partial \mathbf{t}_1^\vartheta} \bar{\Psi}(\ell, \mathbf{t}_1; \lambda) = \frac{\partial^2}{\partial \ell^2} \bar{\Psi}(\ell, \mathbf{t}_1; \lambda) - (4\ell^2 - 2\mathbf{t}_1 + 2)\bar{\Psi}(\ell, \mathbf{t}_1; \lambda), \\ \bar{\Psi}(\ell, 0) = (1 - \lambda) \exp(\ell^2). \end{cases}$$

Case 1. Firstly, take into consideration the CFD coupled with the Shehu homotopy perturbation transform method in the first case of (46). Considering the process stated in Section, we have:

$$\left(\frac{\nu}{\xi}\right)^\vartheta \mathbf{S}[\underline{\Psi}(\ell, \mathbf{t}_1; \lambda)] - \sum_{\kappa=0}^{r-1} \left(\frac{\xi}{\nu}\right)^{\vartheta-\kappa-1} \underline{\Psi}^{(\kappa)}(0) = \mathbf{S}\left[\frac{\partial^2}{\partial \ell^2} \underline{\Psi}(\ell, \mathbf{t}_1; \lambda) - (4\ell^2 - 2\mathbf{t}_1 + 2)\underline{\Psi}(\ell, \mathbf{t}_1; \lambda)\right].$$

Considering the fuzzy initial condition, making use of the inverse Shehu transform implies that:

$$\underline{\Psi}(\ell, \mathbf{t}_1; \lambda) = \frac{\nu}{\xi}(\lambda - 1) \exp(\ell^2) + \mathbf{S}^{-1}\left[\left(\frac{\nu}{\xi}\right)^\vartheta \mathbf{S}\left[\frac{\partial^2}{\partial \ell^2} \underline{\Psi}(\ell, \mathbf{t}_1; \lambda) - (4\ell^2 - 2\mathbf{t}_1 + 2)\underline{\Psi}(\ell, \mathbf{t}_1; \lambda)\right]\right].$$

Now, by implementing the HPM, we have:

$$\sum_{\kappa=0}^{+\infty} \eta^\kappa \underline{\Psi}_\kappa(\ell, \mathbf{t}_1; \lambda) = (\lambda - 1) \exp(\ell^2) + \eta \left(\mathbf{S}^{-1}\left[\left(\frac{\nu}{\xi}\right)^\vartheta \mathbf{S}\left[\left(\sum_{\kappa=0}^{+\infty} \eta^\kappa \underline{\Psi}_\kappa(\ell, \mathbf{t}_1; \lambda)\right)_{\ell\ell} - (4\ell^2 - 2\mathbf{t}_1 + 2)\left(\sum_{\kappa=0}^{+\infty} \eta^\kappa \underline{\Psi}_\kappa(\ell, \mathbf{t}_1; \lambda)\right)\right]\right]\right).$$

By equating the coefficients of same powers of η , we have:

$$\begin{aligned} \eta^0 : \underline{\Psi}_0(\ell, \mathbf{t}_1; \lambda) &= (\lambda - 1) \exp(\ell^2), \\ \eta^1 : \underline{\Psi}_1(\ell, \mathbf{t}_1; \lambda) &= \mathbf{S}^{-1}\left[\left(\frac{\nu}{\xi}\right)^\vartheta \mathbf{S}\left[\left(\underline{\Psi}_0(\ell, \mathbf{t}_1; \lambda)\right)_{\ell\ell} - (4\ell^2 - 2\mathbf{t}_1 + 2)\underline{\Psi}_0(\ell, \mathbf{t}_1; \lambda)\right]\right] = 2(\lambda - 1) \exp(\ell^2) \frac{\mathbf{t}_1^{\vartheta+1}}{\Gamma(\vartheta + 2)}, \\ \eta^2 : \underline{\Psi}_1(\ell, \mathbf{t}_1; \lambda) &= \mathbf{S}^{-1}\left[\left(\frac{\nu}{\xi}\right)^\vartheta \mathbf{S}\left[\left(\underline{\Psi}_1(\ell, \mathbf{t}_1; \lambda)\right)_{\ell\ell} - (4\ell^2 - 2\mathbf{t}_1 + 2)\underline{\Psi}_1(\ell, \mathbf{t}_1; \lambda)\right]\right] \\ &= 4(\lambda - 1)(\vartheta + 2) \exp(\ell^2) \frac{\mathbf{t}_1^{2\vartheta+2}}{\Gamma(2\vartheta + 3)}, \\ \eta^3 : \underline{\Psi}_2(\ell, \mathbf{t}_1; \lambda) &= \mathbf{S}^{-1}\left[\left(\frac{\nu}{\xi}\right)^\vartheta \mathbf{S}\left[\left(\underline{\Psi}_2(\ell, \mathbf{t}_1; \lambda)\right)_{\ell\ell} - (4\ell^2 - 2\mathbf{t}_1 + 2)\underline{\Psi}_2(\ell, \mathbf{t}_1; \lambda)\right]\right] \\ &= 8(\lambda - 1)(\vartheta + 2)(2\vartheta + 3) \exp(\ell^2) \frac{\mathbf{t}_1^{3\vartheta+3}}{\Gamma(3\vartheta + 4)}, \\ &\vdots \end{aligned}$$

The series form solution is presented as follows:

$$\tilde{\Psi}(\ell, \mathbf{t}_1; \lambda) = \tilde{\Psi}_0(\ell, \mathbf{t}_1; \lambda) + \tilde{\Psi}_1(\ell, \mathbf{t}_1; \lambda) + \tilde{\Psi}_2(\ell, \mathbf{t}_1; \lambda) + \tilde{\Psi}_3(\ell, \mathbf{t}_1; \lambda) + \dots,$$

which implies that:

$$\begin{aligned} \underline{\Psi}(\ell, \mathbf{t}_1; \lambda) &= \underline{\Psi}_0(\ell, \mathbf{t}_1; \lambda) + \underline{\Psi}_1(\ell, \mathbf{t}_1; \lambda) + \underline{\Psi}_2(\ell, \mathbf{t}_1; \lambda) + \underline{\Psi}_3(\ell, \mathbf{t}_1; \lambda) + \dots, \\ \bar{\Psi}(\ell, \mathbf{t}_1; \lambda) &= \bar{\Psi}_0(\ell, \mathbf{t}_1; \lambda) + \bar{\Psi}_1(\ell, \mathbf{t}_1; \lambda) + \bar{\Psi}_2(\ell, \mathbf{t}_1; \lambda) + \bar{\Psi}_3(\ell, \mathbf{t}_1; \lambda) + \dots \end{aligned}$$

Finally, we have:

$$\begin{aligned}\underline{\Psi}(\ell, \mathbf{t}_1; \lambda) &= (\lambda - 1) \exp(\ell^2) \left[1 + 2 \frac{\mathbf{t}_1^{\vartheta+1}}{\Gamma(\vartheta+2)} + 4(\vartheta+2) \frac{\mathbf{t}_1^{2\vartheta+2}}{\Gamma(2\vartheta+3)} + 8(\vartheta+2)(2\vartheta+3) \frac{\mathbf{t}_1^{3\vartheta+3}}{\Gamma(3\vartheta+4)} + \dots \right], \\ \bar{\Psi}(\ell, \mathbf{t}_1; \lambda) &= (1 - \lambda) \exp(\ell^2) \left[1 + 2 \frac{\mathbf{t}_1^{\vartheta+1}}{\Gamma(\vartheta+2)} + 4(\vartheta+2) \frac{\mathbf{t}_1^{2\vartheta+2}}{\Gamma(2\vartheta+3)} + 8(\vartheta+2)(2\vartheta+3) \frac{\mathbf{t}_1^{3\vartheta+3}}{\Gamma(3\vartheta+4)} + \dots \right].\end{aligned}$$

Case 2. Now, we employ the ABC derivative operator in the first case of (37) as follows.

Considering the process stated in Section, we have:

$$\frac{\mathbb{B}(\vartheta)}{1 - \vartheta + \vartheta\left(\frac{\nu}{\xi}\right)^\vartheta} \mathbf{S}[\underline{\Psi}(\ell, \mathbf{t}_1; \lambda)] - \frac{\mathbb{B}(\vartheta)}{1 - \vartheta + \vartheta\left(\frac{\nu}{\xi}\right)^\vartheta} \left(\frac{\nu}{\xi}\right) \underline{\Psi}(\ell, 0) = \mathbf{S} \left[\frac{\partial^2}{\partial \ell^2} \underline{\Psi}(\ell, \mathbf{t}_1; \lambda) - (4\ell^2 - 2\mathbf{t}_1 + 2) \underline{\Psi}(\ell, \mathbf{t}_1; \lambda) \right]$$

Considering the fuzzy initial condition, making use of the inverse Shehu transform implies that:

$$\underline{\Psi}(\ell, \mathbf{t}_1; \lambda) = \frac{\nu}{\xi} (\lambda - 1) \exp(\ell^2) + \mathbf{S}^{-1} \left[\frac{1 - \vartheta + \vartheta\left(\frac{\nu}{\xi}\right)^\vartheta}{\mathbb{B}(\vartheta)} \mathbf{S} \left[\frac{\partial^2}{\partial \ell^2} \underline{\Psi}(\ell, \mathbf{t}_1; \lambda) - (4\ell^2 - 2\mathbf{t}_1 + 2) \underline{\Psi}(\ell, \mathbf{t}_1; \lambda) \right] \right].$$

Now, by implementing the HPM, we have:

$$\begin{aligned}\sum_{\kappa=0}^{+\infty} \eta^\kappa \underline{\Psi}_\kappa(\ell, \mathbf{t}_1; \lambda) &= (\lambda - 1) \exp(\ell^2) \\ &+ \eta \left(\mathbf{S}^{-1} \left[\frac{1 - \vartheta + \vartheta\left(\frac{\nu}{\xi}\right)^\vartheta}{\mathbb{B}(\vartheta)} \mathbf{S} \left[\left(\sum_{\kappa=0}^{+\infty} \eta^\kappa \underline{\Psi}_\kappa(\ell, \mathbf{t}_1; \lambda) \right)_{\ell\ell} - (4\ell^2 - 2\mathbf{t}_1 + 2) \left(\sum_{\kappa=0}^{+\infty} \eta^\kappa \underline{\Psi}_\kappa(\ell, \mathbf{t}_1; \lambda) \right) \right] \right] \right).\end{aligned}$$

By equating the coefficients of same powers of η , we have:

$$\begin{aligned}\eta^0 : \underline{\Psi}_0(\ell, \mathbf{t}_1; \lambda) &= (\lambda - 1) \exp(\ell^2), \\ \eta^1 : \underline{\Psi}_1(\ell, \mathbf{t}_1; \lambda) &= \mathbf{S}^{-1} \left[\frac{1 - \vartheta + \vartheta\left(\frac{\nu}{\xi}\right)^\vartheta}{\mathbb{B}(\vartheta)} \mathbf{S} \left[(\underline{\Psi}_0(\ell, \mathbf{t}_1; \lambda))_{\ell\ell} - (4\ell^2 - 2\mathbf{t}_1 + 2) \underline{\Psi}_0(\ell, \mathbf{t}_1; \lambda) \right] \right] \\ &= \frac{(\lambda - 1) \exp(\ell^2)}{\mathbb{B}(\vartheta)} \left[\frac{\vartheta \mathbf{t}_1^{\vartheta+1}}{\Gamma(\vartheta+2)} + (1 - \vartheta) \mathbf{t}_1 \right], \\ \eta^2 : \underline{\Psi}_1(\ell, \mathbf{t}_1; \lambda) &= \mathbf{S}^{-1} \left[\frac{1 - \vartheta + \vartheta\left(\frac{\nu}{\xi}\right)^\vartheta}{\mathbb{B}(\vartheta)} \mathbf{S} \left[(\underline{\Psi}_1(\ell, \mathbf{t}_1; \lambda))_{\ell\ell} - (4\ell^2 - 2\mathbf{t}_1 + 2) \underline{\Psi}_1(\ell, \mathbf{t}_1; \lambda) \right] \right] \\ &= \frac{(\lambda - 1) \exp(\ell^2)}{\mathbb{B}^2(\vartheta)} \left[2\vartheta(\vartheta+2) \frac{\mathbf{t}_1^{2\vartheta+2}}{\Gamma(2\vartheta+3)} + 2(1 - \vartheta) \mathbf{t}_1^2 \right], \\ \eta^3 : \underline{\Psi}_1(\ell, \mathbf{t}_1; \lambda) &= \mathbf{S}^{-1} \left[\frac{1 - \vartheta + \vartheta\left(\frac{\nu}{\xi}\right)^\vartheta}{\mathbb{B}(\vartheta)} \mathbf{S} \left[(\underline{\Psi}_2(\ell, \mathbf{t}_1; \lambda))_{\ell\ell} - (4\ell^2 - 2\mathbf{t}_1 + 2) \underline{\Psi}_2(\ell, \mathbf{t}_1; \lambda) \right] \right] \\ &= \frac{(\lambda - 1) \exp(\ell^2)}{\mathbb{B}^3(\vartheta)} \left[4\vartheta(\vartheta+2)(2\vartheta+3) \frac{\mathbf{t}_1^{3\vartheta+3}}{\Gamma(3\vartheta+4)} + 4(1 - \vartheta) \mathbf{t}_1^3 \right], \\ &\vdots\end{aligned}$$

The series form solution is presented as follows:

$$\tilde{\Psi}(\ell, \mathbf{t}_1; \lambda) = \tilde{\Psi}_0(\ell, \mathbf{t}_1; \lambda) + \tilde{\Psi}_1(\ell, \mathbf{t}_1; \lambda) + \tilde{\Psi}_2(\ell, \mathbf{t}_1; \lambda) + \tilde{\Psi}_3(\ell, \mathbf{t}_1; \lambda) + \dots,$$

which implies that:

$$\begin{aligned}\underline{\Psi}(\ell, \mathbf{t}_1; \lambda) &= \underline{\Psi}_0(\ell, \mathbf{t}_1; \lambda) + \underline{\Psi}_1(\ell, \mathbf{t}_1; \lambda) + \underline{\Psi}_2(\ell, \mathbf{t}_1; \lambda) + \underline{\Psi}_3(\ell, \mathbf{t}_1; \lambda) + \dots, \\ \bar{\Psi}(\ell, \mathbf{t}_1; \lambda) &= \bar{\Psi}_0(\ell, \mathbf{t}_1; \lambda) + \bar{\Psi}_1(\ell, \mathbf{t}_1; \lambda) + \bar{\Psi}_2(\ell, \mathbf{t}_1; \lambda) + \bar{\Psi}_3(\ell, \mathbf{t}_1; \lambda) + \dots.\end{aligned}$$

Finally, we have:

$$\begin{aligned}\underline{\Psi}(\ell, \mathbf{t}_1; \lambda) &= (\lambda - 1) \exp(\ell^2) \left\{ \begin{aligned} &1 + \frac{1}{\mathbb{B}(\vartheta)} \left[\frac{\vartheta \mathbf{t}_1^{\vartheta+1}}{\Gamma(\vartheta+2)} + (1 - \vartheta) \mathbf{t}_1 \right] \\ &+ \frac{1}{\mathbb{B}^2(\vartheta)} \left[2\vartheta(\vartheta + 2) \frac{\mathbf{t}_1^{2\vartheta+2}}{\Gamma(2\vartheta+3)} + 2(1 - \vartheta) \mathbf{t}_1^2 \right] \\ &+ \frac{1}{\mathbb{B}^3(\vartheta)} \left[4\vartheta(\vartheta + 2)(2\vartheta + 3) \frac{\mathbf{t}_1^{3\vartheta+3}}{\Gamma(3\vartheta+4)} + 4(1 - \vartheta) \mathbf{t}_1^3 \right] + \dots, \end{aligned} \right. \\ \bar{\Psi}(\ell, \mathbf{t}_1; \lambda) &= (1 - \lambda) \exp(\ell^2) \left\{ \begin{aligned} &1 + \frac{1}{\mathbb{B}(\vartheta)} \left[\frac{\vartheta \mathbf{t}_1^{\vartheta+1}}{\Gamma(\vartheta+2)} + (1 - \vartheta) \mathbf{t}_1 \right] \\ &+ \frac{1}{\mathbb{B}^2(\vartheta)} \left[2\vartheta(\vartheta + 2) \frac{\mathbf{t}_1^{2\vartheta+2}}{\Gamma(2\vartheta+3)} + 2(1 - \vartheta) \mathbf{t}_1^2 \right] \\ &+ \frac{1}{\mathbb{B}^3(\vartheta)} \left[4\vartheta(\vartheta + 2)(2\vartheta + 3) \frac{\mathbf{t}_1^{3\vartheta+3}}{\Gamma(3\vartheta+4)} + 4(1 - \vartheta) \mathbf{t}_1^3 \right] + \dots. \end{aligned} \right.\end{aligned}\tag{46}$$

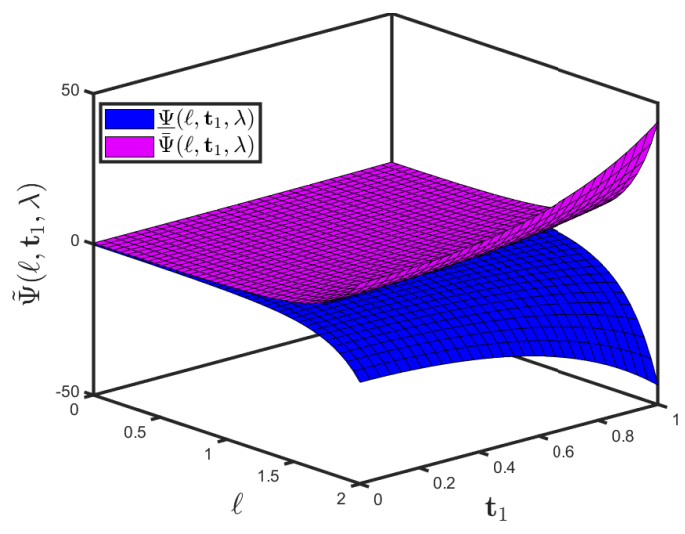
Figure 13a,b reveal how the effectiveness of multiple (lower and upper bound accuracy) surface graphs for Problem 2 interacting with the fuzzy CFD and Shehu transform is being exhibited in this investigation. The pattern specifies the fluctuation in the mapping $\bar{\Psi}(\ell, \mathbf{t}_1; \lambda)$ on the space co-ordinate ℓ with the consideration of \mathbf{t}_1 and the uncertainty parameter $\lambda \in [0, 1]$. The figure illustrates that, as time passes, the mapping $\bar{\Psi}(\ell, \mathbf{t}_1; \lambda)$ will become more intricate.

Figure 14a highlights the impact of the suggested technique on the mapping $\bar{\Psi}(\ell, \mathbf{t}_1; \lambda)$ for the fuzzy CFD to have an uncertainty parameter $\lambda \in [0, 1]$. With the slight increase in $\bar{\Psi}(\ell, \mathbf{t}_1; \lambda)$, it then clearly demonstrates a large decrease in the mapping $\underline{\Psi}(\ell, \mathbf{t}_1; \lambda)$. Figure 14b highlights the effect of the recommended approach on the mapping $\bar{\Psi}(\ell, \mathbf{t}_1; \lambda)$ for the fuzzy CFD to have a fixed fractional order with the varying uncertainty parameter $\lambda \in [0, 1]$. With a small increase in the uncertainty parameter, the mappings $\bar{\Psi}(\ell, \mathbf{t}_1; \lambda)$ and $\underline{\Psi}(\ell, \mathbf{t}_1; \lambda)$ are stable.

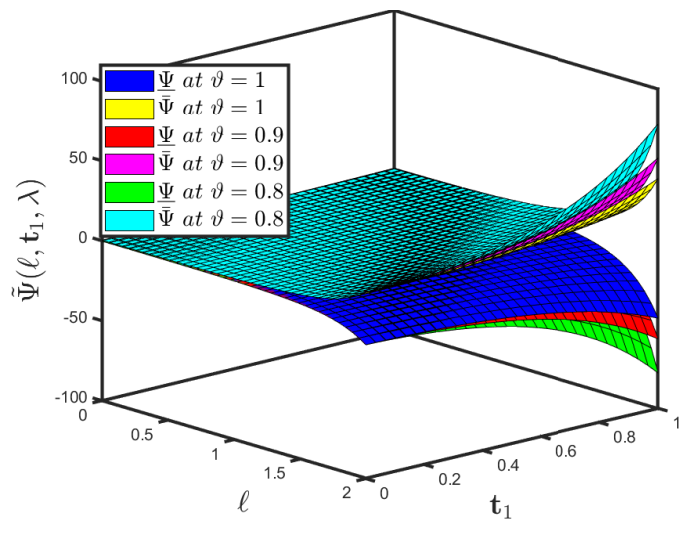
Figure 15a highlights the impact of the suggested technique on the mapping $\bar{\Psi}(\ell, \mathbf{t}_1; \lambda)$ for the fuzzy ABC to have an uncertainty parameter $\lambda \in [0, 1]$. With the slight increase in $\bar{\Psi}(\ell, \mathbf{t}_1; \lambda)$, it then clearly demonstrates a large decrease in the mapping $\underline{\Psi}(\ell, \mathbf{t}_1; \lambda)$. Figure 15b highlights the effect of the recommended approach on the mapping $\bar{\Psi}(\ell, \mathbf{t}_1; \lambda)$ for the fuzzy ABC to have a fixed fractional order with the varying uncertainty parameter $\lambda \in [0, 1]$. With a small increase in the uncertainty parameter, the mappings $\bar{\Psi}(\ell, \mathbf{t}_1; \lambda)$ and $\underline{\Psi}(\ell, \mathbf{t}_1; \lambda)$ are stable.

Figure 16a,b illustrate the comparison between the lower and upper bound accuracies for fuzzy CFD and fuzzy ABC fractional derivative operators for Problem 4 established by the SHPTM for standard motion, i.e., at $\vartheta = 1$.

The graphs in Figures 13–16 assist in recognizing how time and space variation statistically interact. In addition, the proposed method will facilitate scientists' work on pattern formation, diffusion, instability theory, and monitoring competence by employing inferential statistical testing.



(a)



(b)

Figure 13. Three-dimensional plot of $\tilde{\Psi}(\ell, t_1; \lambda)$ of Problem (4): (a) $\underline{\Psi}(\ell, t_1; \lambda)$ and $\bar{\Psi}(\ell, t_1; \lambda)$ when $\vartheta = 1$; (b) $\underline{\Psi}(\ell, t_1; \lambda)$ and $\bar{\Psi}(\ell, t_1; \lambda)$ when the uncertainty parameter $\lambda \in [0, 1]$ has different fractional orders.

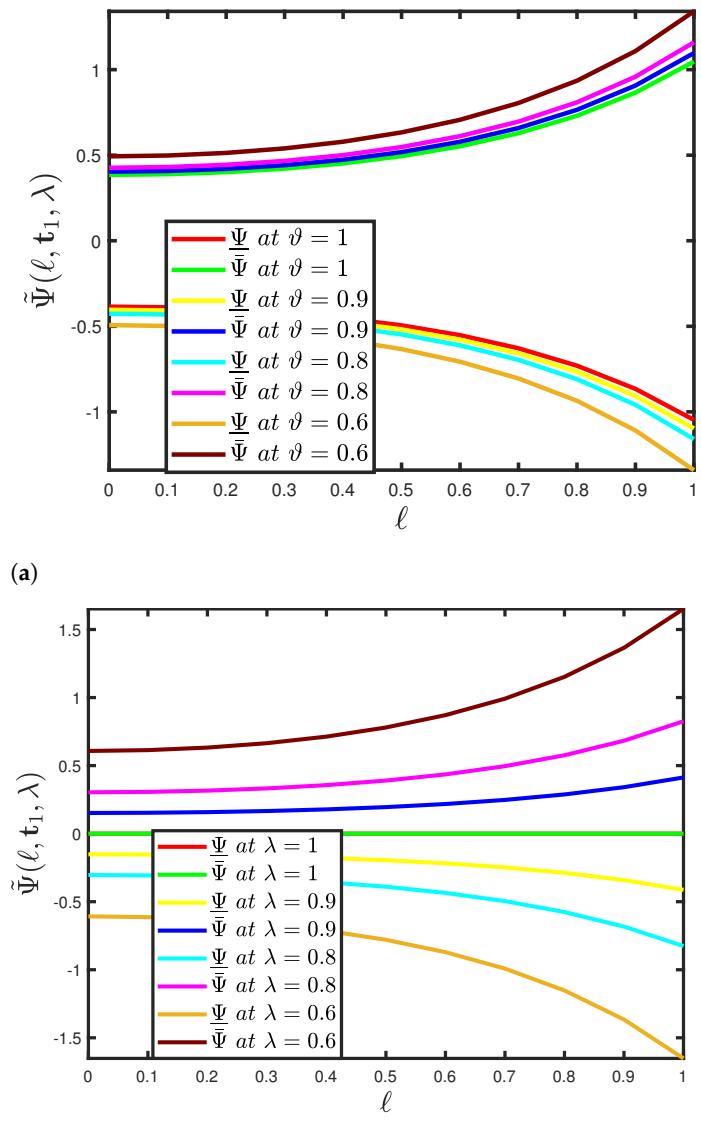
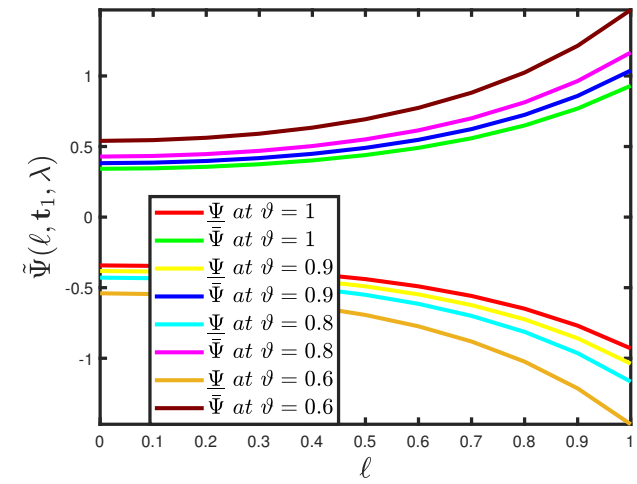
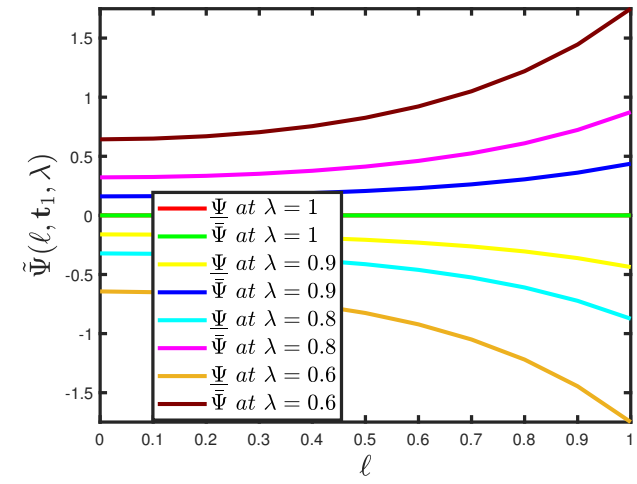


Figure 14. Two-dimensional simulation of $\tilde{\Psi}(\ell, \mathbf{t}_1; \lambda)$ of Problem (4): (a) $\underline{\Psi}(\ell, \mathbf{t}_1; \lambda)$ and $\tilde{\Psi}(\ell, \mathbf{t}_1; \lambda)$ when fuzzy CFD is considered to have an uncertainty parameter $\lambda \in [0, 1]$ and $\mathbf{t}_1 = 0.7$; and (b) $\underline{\Psi}(\ell, \mathbf{t}_1; \lambda)$ and $\tilde{\Psi}(\ell, \mathbf{t}_1; \lambda)$ when fuzzy CFD is considered to have a fractional order $\vartheta = 0.7$ and $\mathbf{t}_1 = 0.7$.

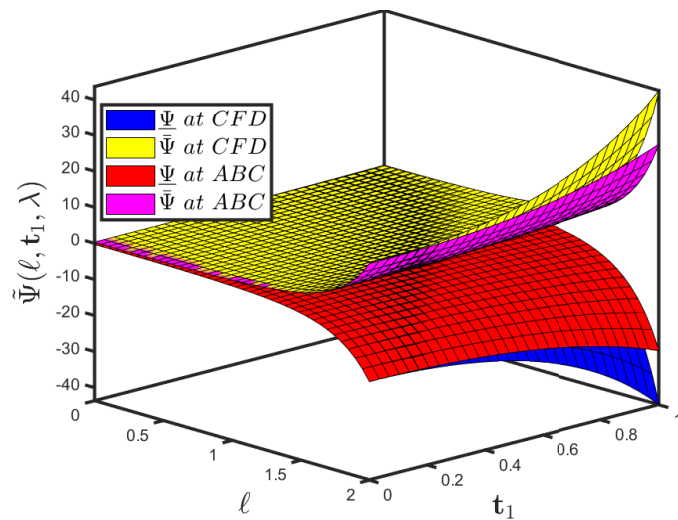


(a)

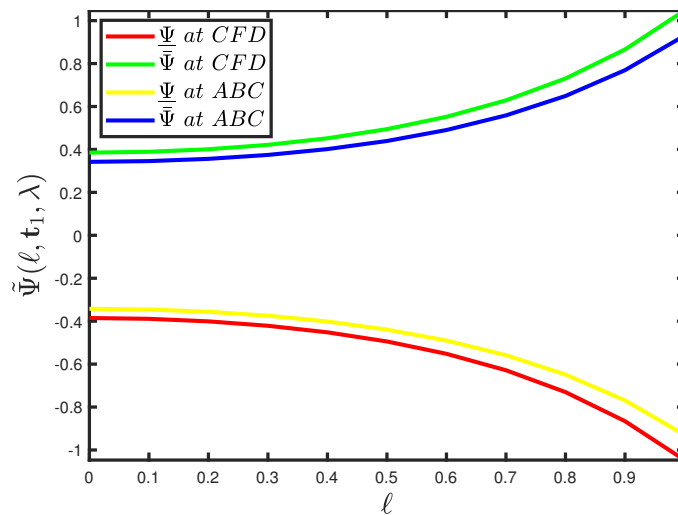


(b)

Figure 15. Two-dimensional simulation of $\tilde{\Psi}(\ell, t_1; \lambda)$ of Problem (4): (a) $\underline{\Psi}(\ell, t_1; \lambda)$ and $\tilde{\Psi}(\ell, t_1; \lambda)$ when fuzzy ABC is considered to have an uncertainty parameter $\lambda \in [0, 1]$ and $t_1 = 0.7$; and (b) $\underline{\Psi}(\ell, t_1; \lambda)$ and $\tilde{\Psi}(\ell, t_1; \lambda)$ when fuzzy ABC is considered to have a fractional order $\vartheta = 0.7$ and $t_1 = 0.7$.



(a)



(b)

Figure 16. Comparison plots of $\tilde{\Psi}(\ell, t_1; \lambda)$ of Problem (4) when fuzzy CFD and ABC are considered to have a fractional order $\vartheta = 1$ and uncertainty parameter $\lambda \in [0, 1]$: (a) three-dimensional plot; (b) two-dimensional plot of $\underline{\Psi}(\ell, t_1; \lambda)$ and $\tilde{\Psi}(\ell, t_1; \lambda)$ when and $t_1 = 0.7$.

Remark 5. When $[\lambda - 1, 1 - \lambda] = 1$ and $\vartheta = 1$, then solution (46) reduces to the integer-order solution $\Psi(\ell, t_1) = \exp(\ell^2 + t_1^2)$.

6. Conclusions

The principal aim of this investigation was to provide an approximate-analytical solution to the fuzzy fractional Cauchy reaction–diffusion equation by taking into consideration the generalized Hukuhara derivative of Caputo and AB fractional derivatives. A stability analysis of the proposed study was presented. The findings will be pertinent in the evaluation of nonlinear complex processes that arise in both scientific disciplines. By employing the fuzzy set theory, this analysis shows that the SHPTM is simple, powerful, adequate, and applicable to a wide range of nonlinear equations. It is remarkable that SHPTM yields solutions in pairs, which often becomes an advantage in selecting the best feasible solution for the governing model. Furthermore, it is clear from graphical views that the approximate findings of ABC operators are in close contact with the CFD operators. When it concerns reducing the size of the computational cost, the SHPTM technique is effective. Because the SHPTM investigates fractional equations without using Adomian's

polynomials, it delivers a wide analytical outcome capacity. This is one of the advantages of the SHPTM method over the decomposition method. Finally, the SHPTM is well suited to all analytical methods and has a wide range of applicability in science and technology.

Author Contributions: Conceptualization and data curation—M.A.A., R.A., S.R., J.S., Z.H., T.A.; formal analysis—M.A.A., R.A., S.R., J.S., Z.H., T.A.; funding acquisition—M.A.A., R.A., S.R., J.S., Z.H., T.A.; investigation—M.A.A., R.A., S.R., J.S., Z.H., T.A.; methodology—M.A.A., R.A., S.R., J.S., Z.H., T.A.; project administration—M.A.A., R.A., S.R., J.S., Z.H., T.A.; supervision—S.R.; resources, software—M.A.A., R.A., S.R., J.S., Z.H., T.A.; validation—M.A.A., R.A., S.R., J.S., Z.H., T.A.; visualization—M.A.A., R.A., S.R., J.S., Z.H., T.A.; writing—original draft—M.A.A., R.A., S.R., J.S., Z.H., T.A.; writing—review & editing—M.A.A., R.A., S.R., J.S., Z.H., T.A. All authors have read and agreed to the published version of the manuscript.

Funding: This research received no external funding.

Institutional Review Board Statement: Not applicable.

Informed Consent Statement: Not applicable.

Data Availability Statement: Not applicable.

Acknowledgments: This research was funded by the Deanship of Scientific Research at Princess Nourah bint Abdulrahman University, Saudi Arabia through the Fast-track Research Funding Program.

Conflicts of Interest: The authors declare no conflict of interest.

References

1. Tarasov, V.E. *Fractional Dynamics: Applications of Fractional Calculus to Dynamics of Particles, Fields and Media*; Springer: Berlin/Heidelberg, Germany, 2010.
2. Uchaikin, V.V. *Fractional Derivatives for Physicists and Engineers*; Springer: Berlin, Germany, 2013.
3. Herrmann, R. *Fractional Calculus: An Introduction for Physicists*, 2nd ed.; World Scientific: Singapore, 2014.
4. Povstenko, Y. *Linear Fractional Diffusion-Wave Equation for Scientists and Engineers*; Birkhäuser: New York, NY, USA, 2015.
5. Caputo, M.; Fabrizio, M. A new definition of fractional derivative without singular kernel. *Progr. Fract. Differ. Appl.* **2015**, *1*, 73.
6. Atangana, A.; Baleanu, D. New fractional derivatives with non-local and non-singular kernel, Theory and Application to Heat Transfer Model. *Therm. Sci.* **2016**, *20*, 2. [[CrossRef](#)]
7. Scherer, R.; Kalla, S. L.; Tang, Y.; Huang, J. The Grünwald-Letnikov method for fractional differential equations. *Comput. Math. Appl.* **2011**, *62*, 3. [[CrossRef](#)]
8. Li, C.; Qian, D.; Chen, Y. Q. On Riemann–Liouville and Caputo Derivatives. *Dis. Dyn. Nat. Soc.* **2011**, *2011*, 562494. [[CrossRef](#)]
9. Morales-Delgado, V.F.; Gómez-Aguilar, J.F.; Yépez-Martínez, H.; Baleanu, D.; Escobar-Jimenez, R.F.; Olivares-Peregrino, V.H. Laplace homotopy analysis method for solving linear partial differential equations using a fractional derivative with and without kernel singular. *Adv. Differ. Equ.* **2016**, *2016*, 164 [[CrossRef](#)]
10. Sheikh, N.A.; Ali, F.; Saqib, M.; Khan, I.; Jan, S.A.A.; Alshomrani, A.S.; Alghamdi, M.S. Comparison and analysis of the Atangana-Baleanu and Caputo-Fabrizio fractional derivatives for generalized Casson fluid model with heat generation and chemical reaction. *Results Phys.* **2017**, *7*, 789. [[CrossRef](#)]
11. Atangana, A.; Alkahtani, B.S.T. New model of groundwater flowing within a confine aquifer: Application of Caputo-Fabrizio derivative. *Arab. J. Geosci.* **2016**, *9*, 1. [[CrossRef](#)]
12. Maitama, S.; Zhao, W. New Laplace-type integral transform for solving steady heattransfer problem. *Therm. Sci.* **2019**, *25*, 1–12. [[CrossRef](#)]
13. Zureigat, H.; Izani, A.I.; Sathasivam, S. Numerical solutions of fuzzy fractional diffusion equations by an implicit finite difference scheme. *Neural Comput. Appl.* **2019**, *31*, 4085–4094. [[CrossRef](#)]
14. Rashid, S.; Kubra, K.T. Fractional spatial diffusion of a biological population model via a new integral transform in the settings of power and Mittag–Leffler nonsingular kernel. *Physica Scripta* **2021**, *96*, 114003. [[CrossRef](#)]
15. Rashid, S.; Ashraf, R.; Akdemir, A. O.; Alqudah, M. A.; Abdeljawad, T.; Mohamed, M. S. Analytic fuzzy formulation of a time-fractional Fornberg–Whitham model with power and Mittag–Leffler kernels. *Fractal Fract.* **2021**, *5*, 113. [[CrossRef](#)]
16. Rashid, S.; Hammouch, Z.; Aydi, H.; Ahmad, A.G.; Alsharif, A.M. Novel computations of the time-fractional Fisher’s model via generalized fractional integral operators by means of the Elzaki transform, *Fractal Fract.* **2021**, *5*, 94. fract5030094. [[CrossRef](#)]
17. Rashid, S.; Kubra, K.T.; Guirao, J.L.G. Construction of an approximate analytical solution for multi-dimensional fractional Zakharov–Kuznetsov equation via Aboodh Adomian decomposition method. *Symmetry* **2021**, *13*, 1542. [[CrossRef](#)]
18. Zhou, S.-S.; Rashid, S.; Rauf, A.; Kubra, K.T.; Alsharif, A.M. Initial boundary value problems for a multi-term time fractional diffusion equation with generalized fractional derivatives in time. *AIMS Math.* **2021**, *6*, 12114–12132. [[CrossRef](#)]

19. Rashid, S.; Jarad, F.; Abualnaja, K.M. On fuzzy Volterra-Fredholm integrodifferential equation associated with Hilfer-generalized proportional fractional derivative, *AIMS Math.* **2021**, *6*, 10920–10946.
20. Rashid, S.; Kubra, K. T.; Rauf, A.; Chu, Y. -M.; Hamed, Y. S. New numerical approach for time-fractional partial differential equations arising in physical system involving natural decomposition method. *Physica Scripta.* **2021**, *96*, 105204. [[CrossRef](#)]
21. Chang, S.S.L.; Zadeh, L. On fuzzy mapping and control. *IEEE Trans. Syst. Man Cybern.* **1972**, *2*, 30–34. [[CrossRef](#)]
22. Zadeh, L.A. The concept of a linguistic variable and its application to approximate reasoning. *Inf. Sci.* **1975**, *8*, 199–249. [[CrossRef](#)]
23. Zadeh, L.A. Linguistic variables, approximate reasoning and disposition. *Med. Inform.* **1983**, *8*, 173–186. [[CrossRef](#)]
24. Negoita, C.V.; Ralescu, D.A. *Applications of Fuzzy Sets to Systems Analysis*; Wiley: New York, NY, USA, 1975. [[CrossRef](#)]
25. Hukuhara, M. Intégration des applications mesurables dont la valeur est un compact convexe. *Funkc. Ekvac.* **1967**, *10*, 205–229.
26. Agarwal, R.P.; Lakshmikantham, V.; Nieto, J.J. On the concept of solution for fractional differential equations with uncertainty, *Nonlinear Anal.* **2020**, *72*, 59–62.
27. Arshad, S.; Lupulescu, V. On the fractional differential equations with uncertainty. *Nonlinear Anal.* **2011**, *74*, 85–93. [[CrossRef](#)]
28. Arshad, S.; Lupulescu, V. Fractional differential equation with fuzzy initial condition. *Elect. J. Diff. Eq.* **2011**, *34*, 1–8. [[CrossRef](#)]
29. Allahviranloo, T.; Salahshour, S.; Abbasbandy, S. Explicit solutions of fractional differential equations with uncertainty. *Soft. Comput.* **2012**, *16*, 297–302.
30. Salahshour, S.; Allahviranloo, T.; Abbasbandy, S. Solving fuzzy fractional differential equations by fuzzy Laplace transforms. *Commun. Nonlin. Sci. Numer. Simul.* **2012**, *17*, 1372–1381. [[CrossRef](#)]
31. Allahviranloo, T.; Abbasbandy, S.; Salahshour, S. Fuzzy fractional differential equations with Nagumo and Krasnoselskii-Krein condition. In Proceedings of the 7th conference of the European Society for Fuzzy Logic and Technology *EUSFLAT-LFA 2011*, Aix-les-Bains, France, 18–22 July 2011. [[CrossRef](#)]
32. Bushnaq, S.; Ullah, Z.; Ullah, A.; Shah, K. Solution of fuzzy singular integral equation with Abel’s type kernel using a novel hybrid method. *Adv. Diff. Eq.* **2020**, *2020*, 156.
33. Ullah, Z.; Ullah, A.; Shah, K.; Baleanu, D. Computation of semi-analytical solutions of fuzzy nonlinear integral equations. *Adv. Diff. Eq.* **2020**, *2020*, 542. [[CrossRef](#)]
34. Salahshour, S.; Ahmadian, A.; Senu, N.; Baleanu, D.; Agarwal, P. On analytical solutions of the fractional differential equation with uncertainty: Application to the Basset problem. *Entropy* **2015**, *17*, 885–902. [[CrossRef](#)]
35. Ahmad, S.; Ullah, A.; Akgül, A.; Abdeljawad, T. Semi-analytical solutions of the 3rd order fuzzy dispersive partial differential equations under fractional operators. *Alex. Eng. J.* **2021**, *60*, 5861–5878. [[CrossRef](#)]
36. Shah, K.; Seadawy, A. R.; Arfan, M. Evaluation of one dimensional fuzzy fractional partial differential equations. *Alex. Eng. J.* **2020**, *59*, 3347–3353. [[CrossRef](#)]
37. Feng, G.; Chen, G. Adaptive control of discrete-time chaotic systems: A fuzzy control approach. *Chaos Solitons Fract.* **2005**, *23*, 459–467. [[CrossRef](#)]
38. Jiang, W.; Guo-Dong, Q.; Bin, D. H1 variable universe adaptive fuzzy control for chaotic system. *Chaos Solitons Fract.* **2005**, *24*, 1075–1086. [[CrossRef](#)]
39. El-Naschie, M. S. A review of E-infinity theory and the mass spectrum of high energy particle physics. *Chaos Solitons Fract.* **2004**, *19*, 209–236. [[CrossRef](#)]
40. Lesnic, D. The decomposition method for Cauchy reaction–diffusion problems. *Appl. Math. Lett.* **2007**, *20*, 412. [[CrossRef](#)]
41. Dehghan, M.; Shakeri, F. Application of He’s variational iteration method for solving the Cauchy reaction–diffusion problem. *J. Comput. Appl. Math.* **2008**, *214*, 435–446. [[CrossRef](#)]
42. Kumar, S.; Kumar, A.; Abbas, S.; Qurashi, M. A.; Baleanu, D. A modified analytical approach with existence and uniqueness for fractional Cauchy reaction-diffusion equations. *Adv. Diff. Equ.* **2020**, *2020*, 28. [[CrossRef](#)]
43. He, J.-H. Homotopy Perturbation Technique. *Comp. Meth. Appl. Mech. Eng.* **1999**, *178*, 257–262. [[CrossRef](#)]
44. He, J. -H. Application of homotopy perturbation method to nonlinear wave equations. *Chaos Solitons Fract.* **2005**, *26*, 695–700. [[CrossRef](#)]
45. He, J. -H. Limit cycle and bifurcation of nonlinear problems. *Chaos Solitons Fract.* **2005**, *26*, 827–833. [[CrossRef](#)]
46. Rashid, S.; Kubra, K.T.; Jafari, H.; Lehre, S.U. A semi-analytical approach for fractional order Boussinesq equation in a gradient unconfined aquifers. *Math. Meth. Appl. Sci.* **2021**. [[CrossRef](#)]
47. Rashid, S.; Kubra, K.T.; Abualnaja, K.M. Fractional view of heat-like equations via the Elzaki transform in the settings of the Mittag–Leffler function. *Math. Meth. Appl. Sci.* **2021**. [[CrossRef](#)]
48. Rashid, S.; Khalid, A.; Sultana, S.; Hammouch, Z.; Shah, R.; Alsharif, A.M. A novel analytical view of time-fractional Korteweg-De Vries equations via a new integral transform. *Symmetry* **2021**, *13*, 1254. [[CrossRef](#)]
49. Allahviranloo, T. *Fuzzy Fractional Differential Operators and Equation Studies in Fuzziness and Soft Computing*; Springer: Berlin, Germany, 2021. [[CrossRef](#)]
50. Zimmermann, H.J. *Fuzzy Set Theory and Its Applications*; Kluwer Academic Publishers: Dordrecht, The Netherlands, 1991.
51. Zadeh, L.A. Fuzzy sets. *Infor. Cont.* **1965**, *8*, 338–353.
52. Allahviranloo, T.; Ahmadi, M.B. Fuzzy Laplace Transform. *Soft Comput.* **2010**, *14*, 235–243. [[CrossRef](#)]
53. Maitama, S.; Zhao, W. Homotopy analysis Shehu transform method for solving fuzzy differential equations of fractional and integer order derivatives. *Comput. Appl. Math.* **2021**, *40*, 86. [[CrossRef](#)]

54. Maitama, S.; Zhao, W. New integral transform: Shehu transform a generalization of Sumudu and Laplace transform for solving differential equations. *Int. J. Anal. Appl.* **2019**, *17*, 167–190. [[CrossRef](#)]
55. Bokhari, A.; Baleanu, D.; Belgacema, R. Application of Shehu transform to Atangana-Baleanu derivatives, *J. Math. Comp. Sci.* **2020**, *20*, 101–107.
56. Ghorbani, A. Beyond Adomian polynomials: He polynomials. *Chaos Solitons Fract.* **2009**, *39*, 1486–1492. [[CrossRef](#)]
57. Hamoud, A.; Ghadle, K. Modified Adomian decomposition method for solving fuzzy Volterra—Fredholm integral equations. *J. Indian Math. Soc.* **2018**, *85*, 52–69. [[CrossRef](#)]
58. Osman, M.; Gong, Z.; Mustafa, A.M.; Yang, H. Solving fuzzy (1+n)-dimensional Burgers' equation. *Adv. Diff. Equ.* **2021**, *2021*, 219. [[CrossRef](#)]